POWER AUTHORITY OF THE STATE OF NEW YORK

10 COLUMBUS CIRCLE NEW YORK. N. Y. 10019

(212) 397-6200

January 26, 1983
JPN-83-07

Director of Nuclear Reactor Regulation
U.S. Nuclear Regulatory Commission
Washington, D.C. 20555

Attention: Mr. Domenic B. Vassallo, Chief
            Operating Reactors Branch No. 2
            Division of Licensing

Subject: James A. FitzPatrick Nuclear Power Plant
            Docket No. 50-333
            Core Spray "A" Metallurgical Analysis

References: 1. Letter, J.P. Bayne (PASNY) to D.B. Vassallo
                (NRC) dated October 15, 1982 (JPN-82-79)

            2. Letter, J.P. Bayne (PASNY) to I.A. Ippolito
                (NRC) dated January 20, 1982 (JPN-82-12)

Dear Sir:

As reported in references 1 and 2, a rejectable indication
was found in the stainless steel (Type 304) portion of the
"A" core spray header. This section of piping (from the
reactor pressure vessel to the first isolation valve) was
removed and replaced with 316L grade stainless steel.

That portion of the piping containing the rejectable
indication was subsequently sent to Battelle Columbus Laboratories
(BCL) for metallurgical analysis. Attachments 1 and 2 are
the reports of that analysis dated March 25, and July 30,
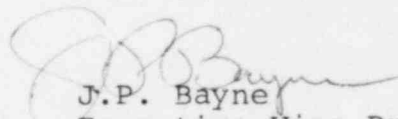1982 respectively.

A001

These reports are submitted for your information. The following conclusions are of particular interest:

1. The initiation of the discovered intergranular cracking resulted from the presence of fabrication-induced surface flaws.

2. Cracking occurred only in conjunction with the fabrication-induced surface flaws.

3. There appears to have been limited crack branching.

4. The cracking appears to have been arrested upon reaching the weld metal.

Additionally, it should be noted that this cracking was discovered by ultrasonic examination, using a dual probe, 45° shear wave technique. This method was used to examine other portions of the stainless steel piping at FitzPatrick during the 1981 refueling outage and is planned for use during the 1983 refueling outage.

Should you require any additional information, please do not hesitate to contact J.A. Gray, Jr. of my staff.

Very truly yours,

J.P. Bayne
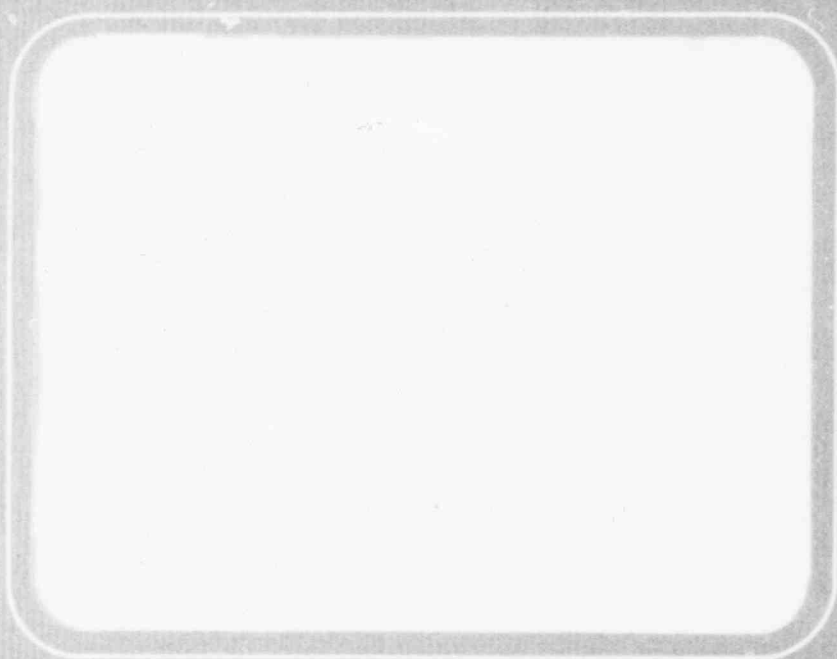Executive Vice President
Nuclear Generation

cc: Mr. J. Linville
     Resident Inspector
     U.S. Nuclear Regulatory Commission
     P.O. Box 136
     Lycoming, NY   13093

Battelle

Columbus Laboratories

Report

SUMMARY REPORT

on

A METALLOGRAPHIC INVESTIGATION OF A
TYPE 304 STAINLESS STEEL SCHEDULE 80 PIPE

to

POWER AUTHORITY OF THE STATE OF NEW YORK
JAMES A. FITZPATRICK NUCLEAR POWER PLANT

March 25, 1982

by

R. D. Buchheit

BATTELLE
Columbus Division
505 King Avenue
Columbus, Ohio 43201

March 25, 1982

Mr. A. V. Sorentino
Power Authority of the
  State of New York
10 Columbus Circle
New York, New York 10019

Dear Mr. Sorentino:

Enclosed are ten copies of our summary report entitled "A Metallographic Investigation of a Type 304 Stainless Steel Schedule 80 Pipe". This report describes the details of our investigation as proposed in our letters of December 18 and December 30, 1981, and the results obtained.

Briefly, the results of the investigation indicated that one of numerous linear defects observed on the inside surface of the subject pipe was the site of a fabrication-induced surface flaw. Although this defect apparently was not the indication believed to have been detected by the Power Authority of the State of New York using an ultrasonic nondestructive-detection technique, it was adjacent to it. The surface flaw appeared to be a lap or fold that probably occurred during the piercing or other operation in the process of producing the seamless pipe. However, the surface flaw apparently was a major contributor to the initiation of an intergranular stress-corrosion crack that propagated from the base of the flaw through about 77 percent of the thickness of the pipe wall.

During our meeting with the Messers. John Boardman and David Sancic on February 18, we discussed the need for additional investigative work concerning the linear defects and cracking. In particular, other linear defects located away from the weld should be examined.

We have enjoyed performing the subject metallographic investigation, and we look forward to a continuation of the investigation. If you have any questions concerning our work or the results obtained, please feel free to contact me.

Very truly yours,

R. D. Buchheit

RDB:rw

TABLE OF CONTENTS

LIST OF FIGURES

A METALLOGRAPHIC INVESTIGATION OF A
TYPE 304 STAINLESS STEEL SCHEDULE 80 PIPE

by

R. D. Buchheit

INTRODUCTION

A part of the core-spray system for a boiling-water reactor at the James A. Fitzpatrick Nuclear Power Plant of the Power Authority of the State of New York (PASNY) was constructed of 12-inch-diameter Type 304 stainless steel Schedule 80 seamless pipe. The core-spray system, which contained stagnant water at a temperature of about 545 F and a pressure of 1005 psig, was placed in service in July, 1975.

After approximately 6 years of service that included intermittent pipe inspections, an inspection of the pipe by nondestructive ultrasonic-inspection techniques detected the presence of a linear defect of unknown type. The linear ultrasonic indication was located on the inside surface of a straight section of the pipe adjacent to a circumferential weld that joined the straight pipe section to an elbow section. The indication was reported to be about 1-3/8 inches long, in close proximity and oriented perpendicular to the weld (i.e., parallel to the longitudinal axis of the pipe). From the nature of the indication, the defect probably had not penetrated the weld metal.

The PASNY was concerned about the nature of the defect that was detected ultrasonically. In particular, if the defect were a crack, it was important to know whether or not the crack exhibited characteristics common to stress-corrosion cracking (SCC). Consequently, PASNY requested that Battelle's Columbus Laboratories (BCL) conduct a metallographic investigation to identify, insofar as possible within the limits of the study, the nature of the linear surface defect that had been detected ultrasonically. The procedure used and results of the investigation conducted by BCL are described in this report.

SUMMARY

Macroscopic examination of the inside surface of a 12-inch-diameter Type 304 stainless steel seamless pipe revealed the presence of numerous linear defects in addition to one that was detected by PASNY using nondestructive ultrasonic-inspection techniques. A cross section through one of the linear defects that was located close to a weld was examined metallographically. The results of the examination indicated that the linear defect was most likely a fabrication-induced surface flaw that resembled a lap or seam. The surface flaw apparently acted as a stress raiser and in the presence of a corrosive environment (the water contained in the pipe), and under the influences of hoop stresses induced by the internal pressure and possibly residual stresses in the hoop direction, it led to the initiation and propagation of an intergranular stress corrosion crack through a sensitized region in the weld heat-affected zone.

PROCEDURE

The photograph in Figure 1 shows a portion of the Type 304 stainless steel pipe that contained the linear indication detected by PASNY, that was submitted to BCL for the investigation. That portion of the pipe was approximately 15 inches long; it included about 7 inches of the straight-pipe section and about 7 inches of the elbow section that were joined together by the circumferential weld.

Figure 1 shows the welded pipe sections after decontamination treatments were performed at BCL. Due to the high level of radiation from the surfaces of the welded pipe section upon receipt at BCL, the pipe section was decontaminated by immersion for 1 to 2 hours at 200 F in a solution that consisted of 100 g of sodium hydroxide and 30 g of potassium permanganate dissolved in 1000 cc of water, followed by immersion for 1 to 2 hours at 200 F in a solution that consisted of 100 g of ammonium citrate dissolved in 100 cc of water. After the two immersion treatments, the pipe section was rinsed in water and dried in air. This entire procedure was repeated several times until the radiation level was reduced to about 4 mR/hr on

~1/4X   C9643
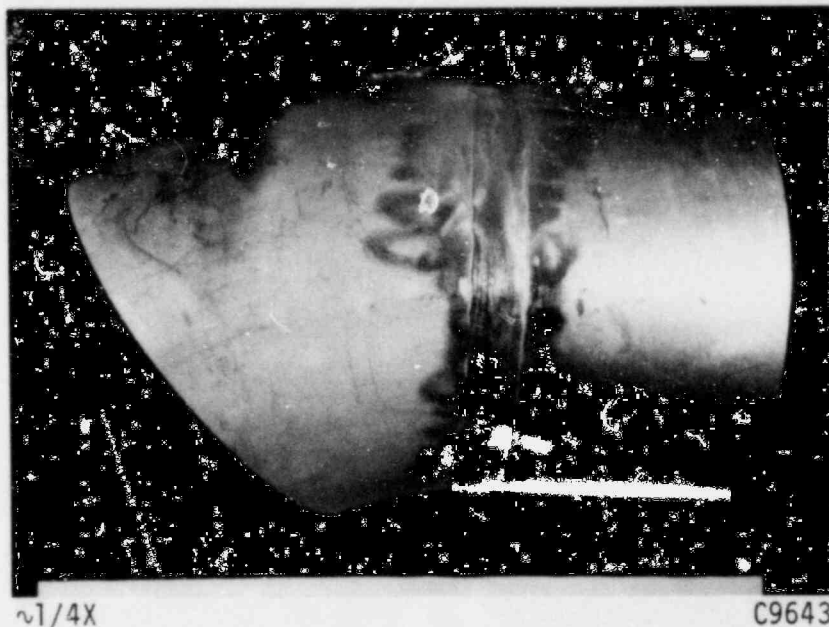
FIGURE 1.   PORTION OF THE TYPE 304 STAINLESS STEEL
            PIPE FROM THE REACTOR CORE-SPRAY SYSTEM
            THAT CONTAINED THE LINEAR INDICATION
            DETECTED ULTRASONICALLY

contact. That level of radiation permitted the entire metallographic in-
vestigation to be performed using "cold" metallographic-laboratory
facilities.

     Subsequent to decontamination , three different regions that con-
tained defects were visible to the unaided eye on the inside surface of the
straight-pipe section. A dye-penetrant inspection of the inside surface
did not produce any indications of linear defects that were not observed
visually. One of the regions of the inside surface that contained the linear
defects and the linear indication obtained ultrasonically by PASNY was re-
moved from the welded pipe section by sectioning and was examined
metallographically.

EXAMINATIONS AND RESULTS

Macroscopic Examinations

The photograph in Figure 2 reveals two regions on the inside surface of the pipe that contained linear surface defects. The defects are only faintly visible in Figure 2; a few of the defects are denoted by small arrows. Note that the two regions were essentially aligned parallel to each other, but were oriented at a small angle to the axial direction.

Circumferential weld

~3/10X   C9829
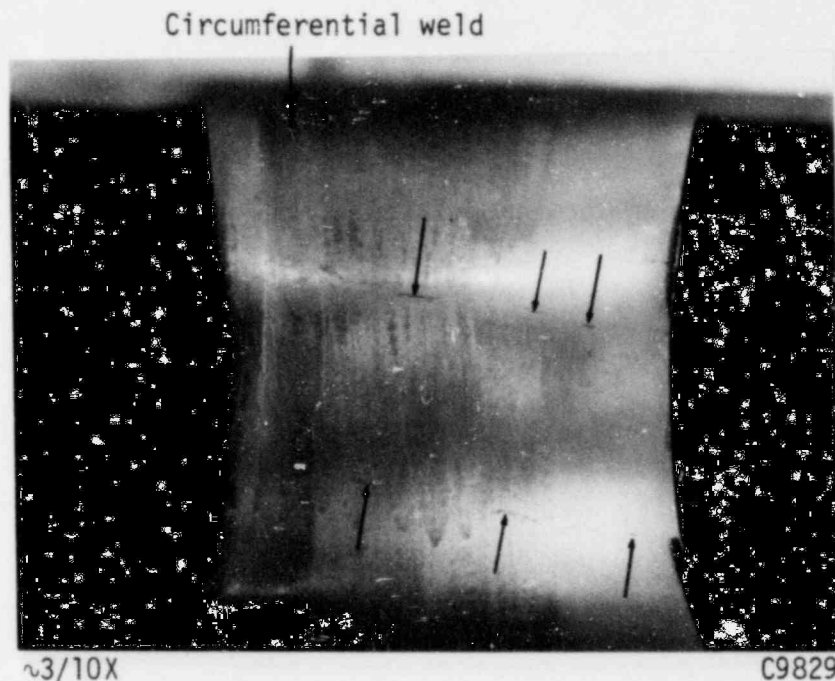
FIGURE 2.   TWO REGIONS THAT CONTAINED LINEAR
            DEFECTS ON THE INSIDE SURFACE
            OF THE PIPE

The region of the inside pipe surface that was subjected to metallographic examinations was located about 180 degrees from the portion of the surface shown in Figure 2. A photograph of that surface is shown in Figure 3. Linear defects were observed at the locations of the unlabeled

Root pass of the circumferential weld

FIGURE 3. LINEAR DEFECTS OBSERVED ON THE INSIDE SURFACE OF THE STRAIGHT-PIPE SECTION

The arrows identify the linear defects.

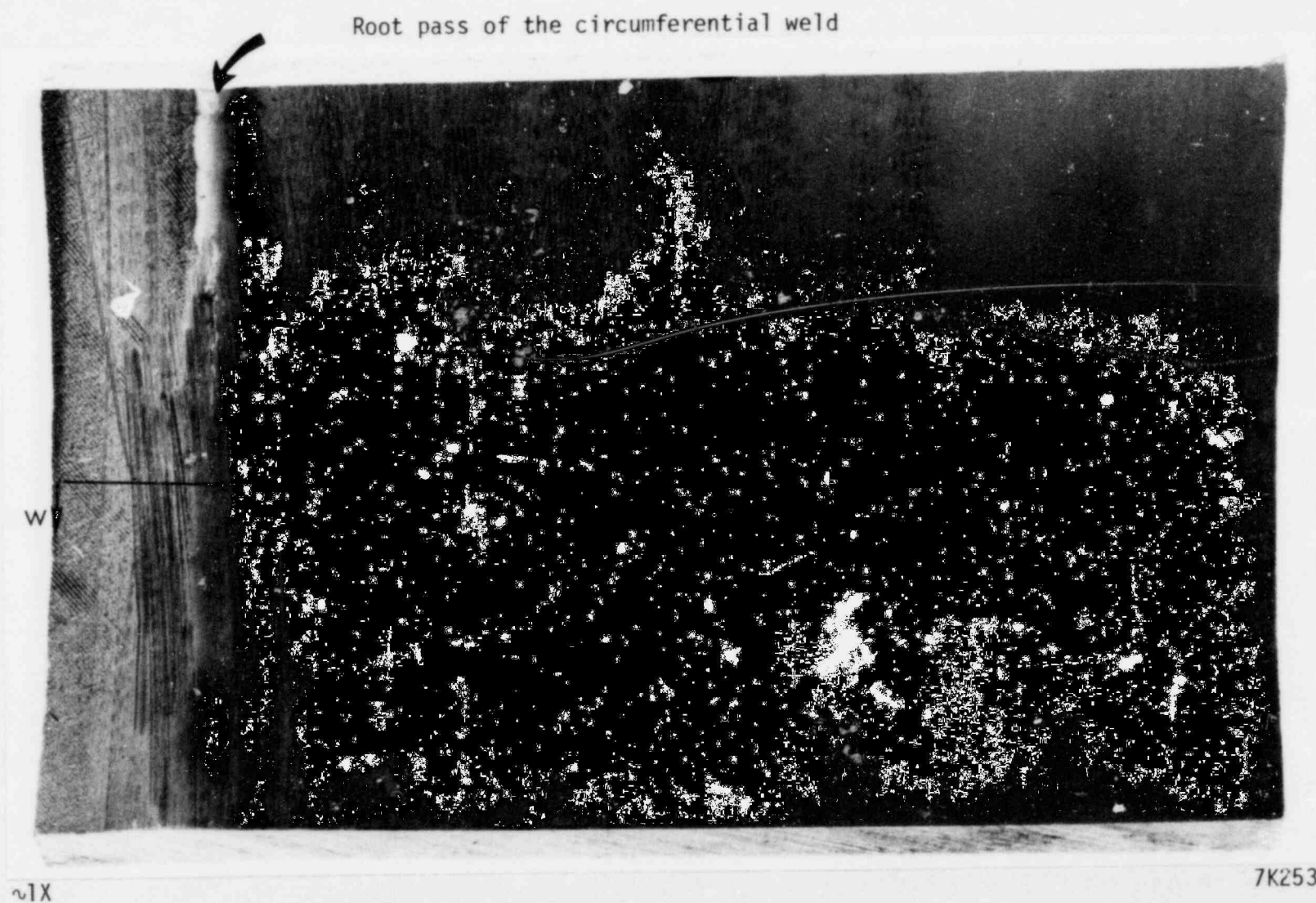arrows and, also at the locations of Arrows 1 and 2 in Figure 3. Approximately 20 separate surface defects were visible at magnifications up to 30X. Three of those linear surface defects were very close to the root pass of the weld. The general orientations of the defects were not axial; they were oriented at an angle of about 10 degrees to the axial direction. This orientation was essentially parallel to the defects in the two regions in Figure 2. Associated with the linear defects, other surface imperfections that appeared to be evidence of thin slivers of surface metal that had been removed or lost were observed at the three locations denoted H in Figure 3. At the location of Arrow E, there appeared to be a thin sliver of surface metal that had been lifted, but not removed, from the surface, The slivers appeared to have resulted from mechanical deformation of surface metal in the direction from the bottom toward the top in Figure 3. At a magnification of 30X the more prominent linear defects also appeared to have been formed by deformation of surface metal in the same direction, i.e., those linear defects had the appearance of surface folds or laps. A minority of the linear defects were tight, hairline indications; macroscopic examination suggested that they were cracks.

The length of the linear defects that were observed varied from about 0.06 to about 1.56 inches. The linear defect at the location of Arrow 2 in Figure 3 was about 1.37 inches long. That defect apparently corresponded in location and length to the indication that was obtained during the ultrasonic, nondestructive inspection by PASNY.

Figure 3 also reveals evidence that the region of the inside surface of the pipe that contained the linear defects had been ground mechanically or abraded. The abraded area covered part of the root pass of the weld and extended for about 4 inches from the weld. With proper illumination on the abraded surface, the surface appeared to have been abraded slightly deeper along the linear defect located at Arrow 2 than over the remainder of the surface in the abraded region. That appearance is barely discernible in Figure 3 because of problems in illuminating the specimen so as to reveal all of the features in one photograph. This observation suggests that a purposeful attempt was made at some time after welding to remove observed surface imperfections, particularly the linear defect that probably was detected later ultrasonically and marked by Arrow 2 in Figure 3.

Examination of the Weld

A metallographic cross section of the weld, Section W-W in Figure 3, was prepared for microscopic examination to determine if the weld heat-affected zone in the straight-pipe section had been sensitized. The cross section was located about 1/4 inch from the linear defect identified by Arrow 1 in Figure 3. The specific objective in examining the weld cross section was to determine the approximate location of a sensitized zone, if one were present, so that the location of the zone could be translated to the linear defect of Arrow 1 and a cross section of that defect could be made within the sensitized zone.

A photomacrograph of the cross section of the weld is presented in Figure 4. The root pass of the weld identifies the inside surface of the pipe. Microscopic examination revealed that sensitized material was present principally in the straight section in the heat-affected zone that was adjacent to the root pass. The degree of sensitization appeared to be

Outside

Inside

4X   Etched   7K252
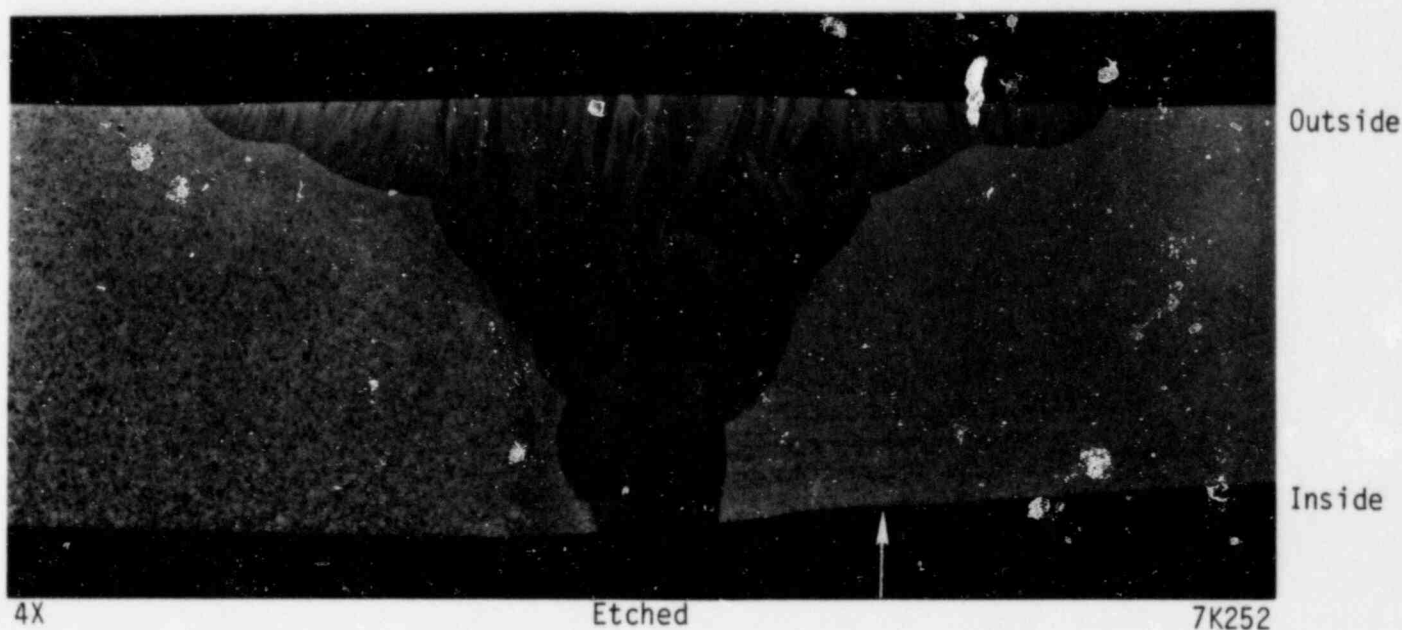
FIGURE 4.   CIRCUMFERENTIAL WELD BETWEEN THE ELBOW SECTION (LEFT) AND
            THE STRAIGHT SECTION (RIGHT) OF THE TYPE 304 STAINLESS
            STEEL SCHEDULE 80 PIPE

The cross section is identified as Section W-W in Figure 3.

mild based on the apparent size and concentration of the carbide precipi-
tates in the austenite grain boundaries. The sensitization appeared to
become considerably less severe towards the outside pipe surface. At the
inside surface, the midregion of the sensitized zone was at the approximate
location of the arrow in Figure 4. That location was translated to
Section S-S (shown in Figure 3) across the linear defect marked by Arrow 1.

## Examination of a Linear Defect

A cross section at Section S-S of the linear defect marked by
Arrow 1 in Figure 3 was prepared metallographically for microscopic exami-
nations. Section S-S was located about 0.19 inch from the visible end of the
defect closest to the weld. As was noted above, that cross section with
respect to the weld corresponded to the approximate location of the arrow
in Figure 4. At that location, the cross section intersected the top
passes of the weld in the outside surface of the pipe.

The metallographic cross section of the linear defect is shown in
the as-polished condition in Figure 5a. The cross section revealed the
presence of a crack that was perpendicular to the surface of the pipe. The
crack extended from a location about 0.010 inch below the inside pipe sur-
face for a distance through the pipe wall of about 0.41 inch. The wall
thickness of the pipe at that cross section was about 0.53 inch; thus, the
crack extended through approximately 77 percent of the pipe wall. As is
shown in Figure 5c, the crack propagated into weld metal for a distance of
about 0.027 inch and then terminated. In the weld heat-affected zone,
crack propagation occurred entirely along the boundaries of equiaxed
austenite grains; in the fusion zone, the crack continued to propagate
along the austenite grain boundaries of the weld metal. Intergranular
branching cracks were numerous along the entire length of the crack, although
fewer branching cracks were observed within the weld metal. It appeared as
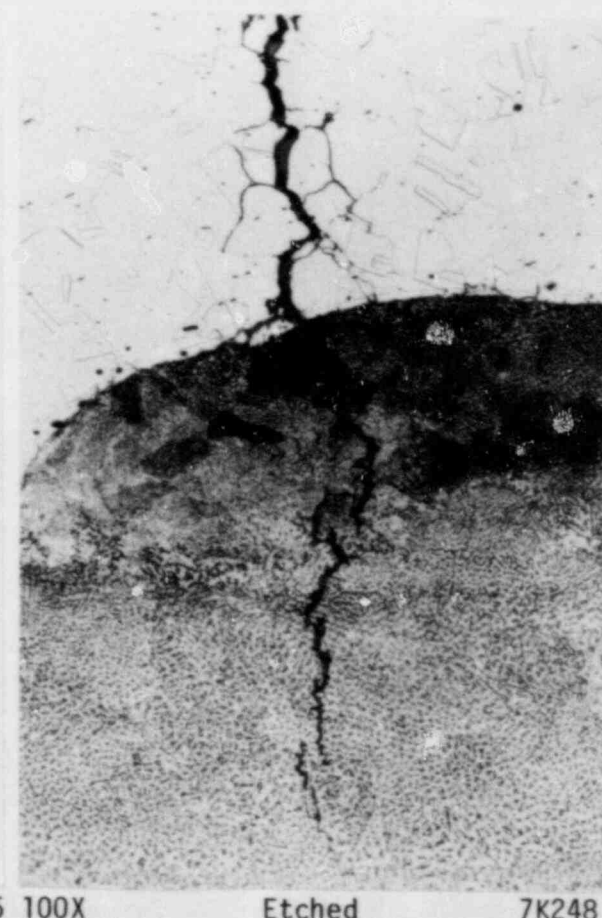though crack propagation may have been arrested by the weld metal.

The as-polished appearance of the linear defect in the inside
surface of the pipe in this cross section is shown in Figure 6, which is
Circled Area 2 in Figure 5a at a higher magnification. The surface defect

Inside pipe surface

| 7X | As Polished | 7K242 | 100X | As Polished | 7K245 | 100X | Etched | 7K248 |
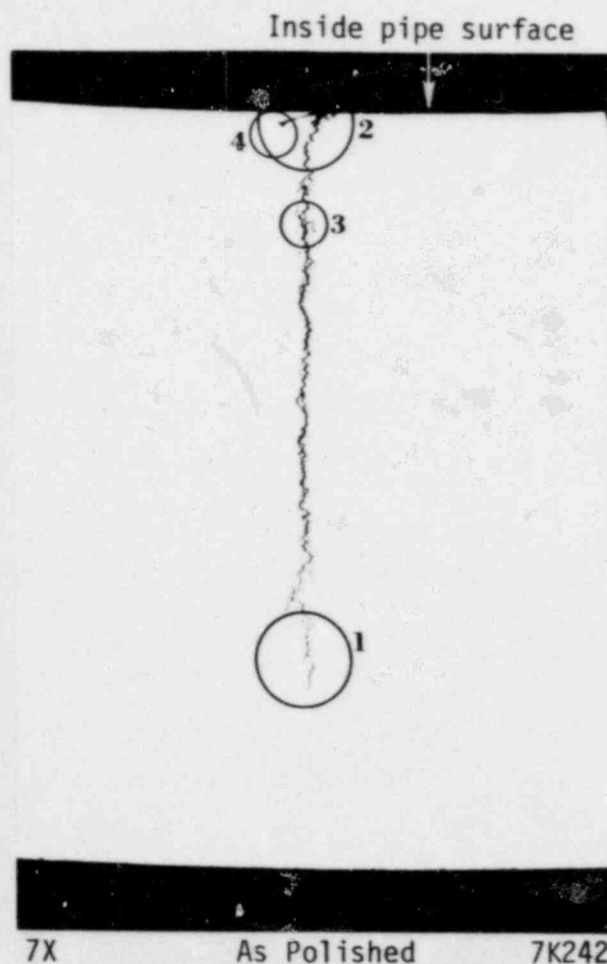
a. Crack in the Pipe Wall
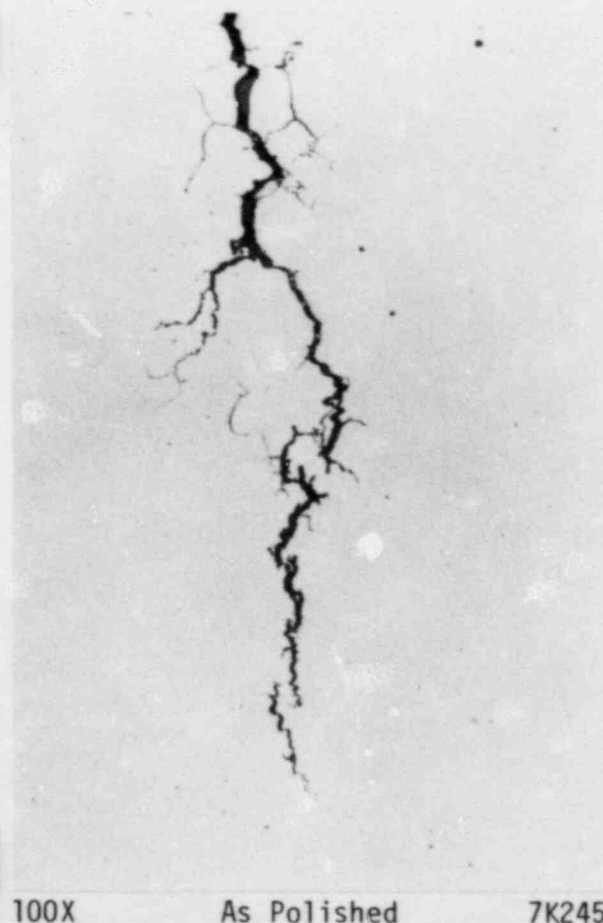
b. Circled Area 1 in (a) at a Higher Magnification

c. Same Field as (b) After Etching Electrolytically in 10% Oxalic Acid

FIGURE 5.   CRACK OBSERVED IN THE CROSS SECTION THROUGH THE LINEAR SURFACE DEFECT MARKED BY ARROW 1 IN FIGURE 3
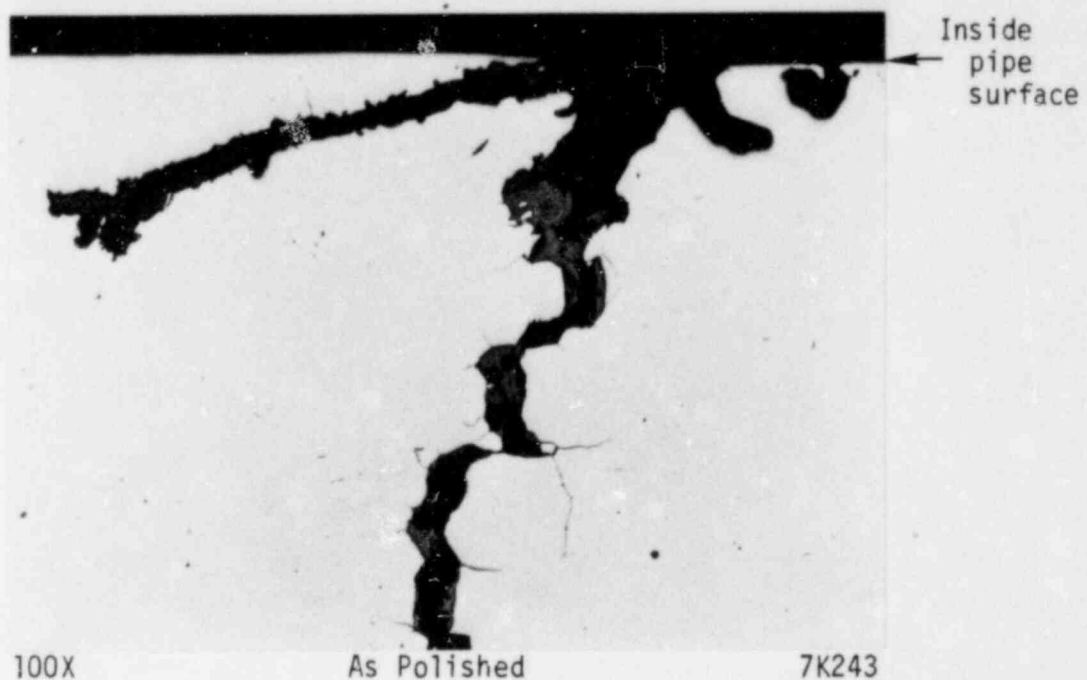
9

100X As Polished 7K243

FIGURE 6. CROSS SECTION OF THE LINEAR DEFECT
WITHIN CIRCLED AREA 2 IN FIGURE 5a

at which the crack initiated seemed to extend to a depth of about 0.010
inch below the surface and did not appear to be an intergranular crack.
Rather than exhibiting characteristics of an intergranular crack, the
defect exhibited characteristics similar to those generally observed for
seams or laps in billet surfaces. For example, an apparent overlap, or
fold, of surface metal that contained what appears to be oxide at the
interface is evident in Figure 6 to the left of the part that showed on
the pipe surface. The start of intergranular cracking was apparent only
at a depth of about 0.010 inch (the depth of the lap and associated pit)
below the surface.

A typical region of the intergranular crack is shown in Figure 7.
That region is within Circled Area 3 in Figure 5a. A dense nonmetallic
corrosion product that can be seen in Figure 7 was observed on the princi-
pal crack surfaces and in adjacent grain boundaries where crack branching

250X   As Polished   7K246

FIGURE 7.   TYPICAL REGION OF THE INTERGRANULAR
            CRACK THAT WAS LOCATED WITHIN
            CIRCLED AREA 3 IN FIGURE 5a

occurred. The crack was nearly filled with the corrosion product near,
and at the tip (see Figure 5b).

Sensitization was revealed in the cross section through the defect
by electrolytic etching using an electrolyte that consisted of 10 percent by
weight of oxalic acid in water. (This is an etch commonly used to reveal a
sensitized microstructure in stainless steels.) Evidence of sensitization,
the presence of fine carbide precipitates in the austenite grain boundaries,
is presented in Figure 8. The area shown in Figure 8 was located within
Circled Area 4 in Figure 5a. The presence of sensitized material was

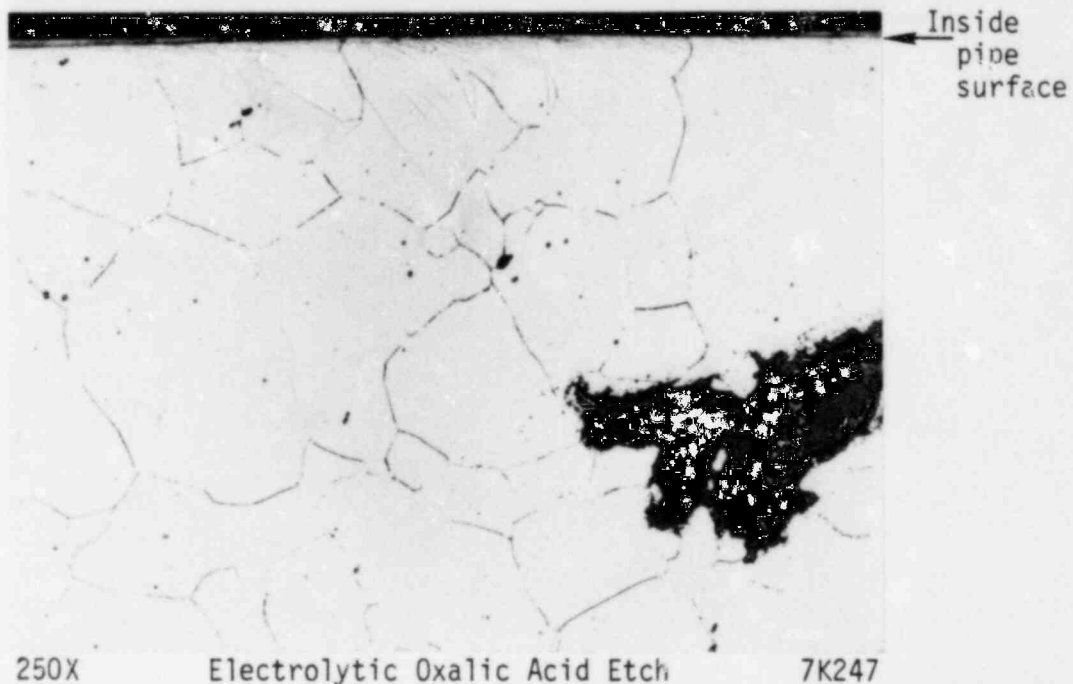250X   Electrolytic Oxalic Acid Etch   7K247

FIGURE 8.   SENSITIZATION (CARBIDE PRECIPITATE IN THE
GRAIN BOUNDARIES) OBSERVED IN THE REGION
OF THE LINEAR SURFACE DEFECT

Circled Area 4 in Figure 5a.

revealed clearly by the etch to a depth of about 0.20 inch below the inside
surface of the pipe. Beyond that depth, evidence of sensitization was
observed in random grain boundaries.

Figure 8 also shows evidence of some cold working of the metal
at the inside pipe surface. Strain lines and deformation that indicated
cold working can be seen faintly in Figure 8 in grains at the pipe surface.
The cold-worked surface metal was most likely a result of the mechanical
surface grinding or abrasion that was evident.

In addition to the sensitizied region, the cold-worked surface
metal, and the intergranular cracking that was revealed in the micro-
structure by etching, the etched microstructure also revealed a flow pat-
tern of the metal that develped during the fabrication of the pipe. The

flow pattern was manifested by coring in the microstructure that had per-
sisted through all of the fabrication steps during the production of the
seamless pipe from the ingot. Coring is interdendritic solid-solution alloy
segregation that originates during the solidification of the ingot. In
essence, coring is chemical inhomogenity in the material that affects the
rate of attack by etching reagents. The rate of attack of some reagents
might be affected more than that of other reagents. The coring in the sub-
ject pipe had a significant effect on the rate of attack of the electrolytic
oxalic acid etchant that was used to reveal sensitized material. The coring
that was revealed by the etchant in the cross section of the linear surface
defect is exhibited in Figure 9 as wavy striations or bands. The striations,
which were actually alternate ridges and grooves in the etched surface, were
enhanced for photography by the use of Nomarski interference-contrast
microscopy.

The coring pattern in Figure 9 shows that an interruption of the
normal flow of metal occurred around the linear defect in the surface of the
pipe during fabrication. The flow pattern around the linear defect was similar
to that sometimes observed around seams or laps in billet surfaces. However,
inasmuch as the linear defect was on the inside surface of seamless pipe,
the origin of the linear defect must have been associated with the piercing
or other operation in the process of producing the seamless pipe.

Note in Figure 9 that the cored regions were independent of the
grains and the grain boundaries and that the coring had no noticeable effect
on the initiation or propagation of the crack.

DISCUSSION

The metallographic investigation revealed the presence of a signi-
ficant number of linear defects on the inside surface of the pipe, in
addition to the linear defect that was detected by PASNY using a nondestruc-
tive ultrasonic inspection technique. The linear defect chosen for metal-
lographic examination in cross section was probably not the exact indication
that was obtained ultrasonically, but was adjacent to it. The results of
the examination of the selected defect indicated that, at the inside pipe
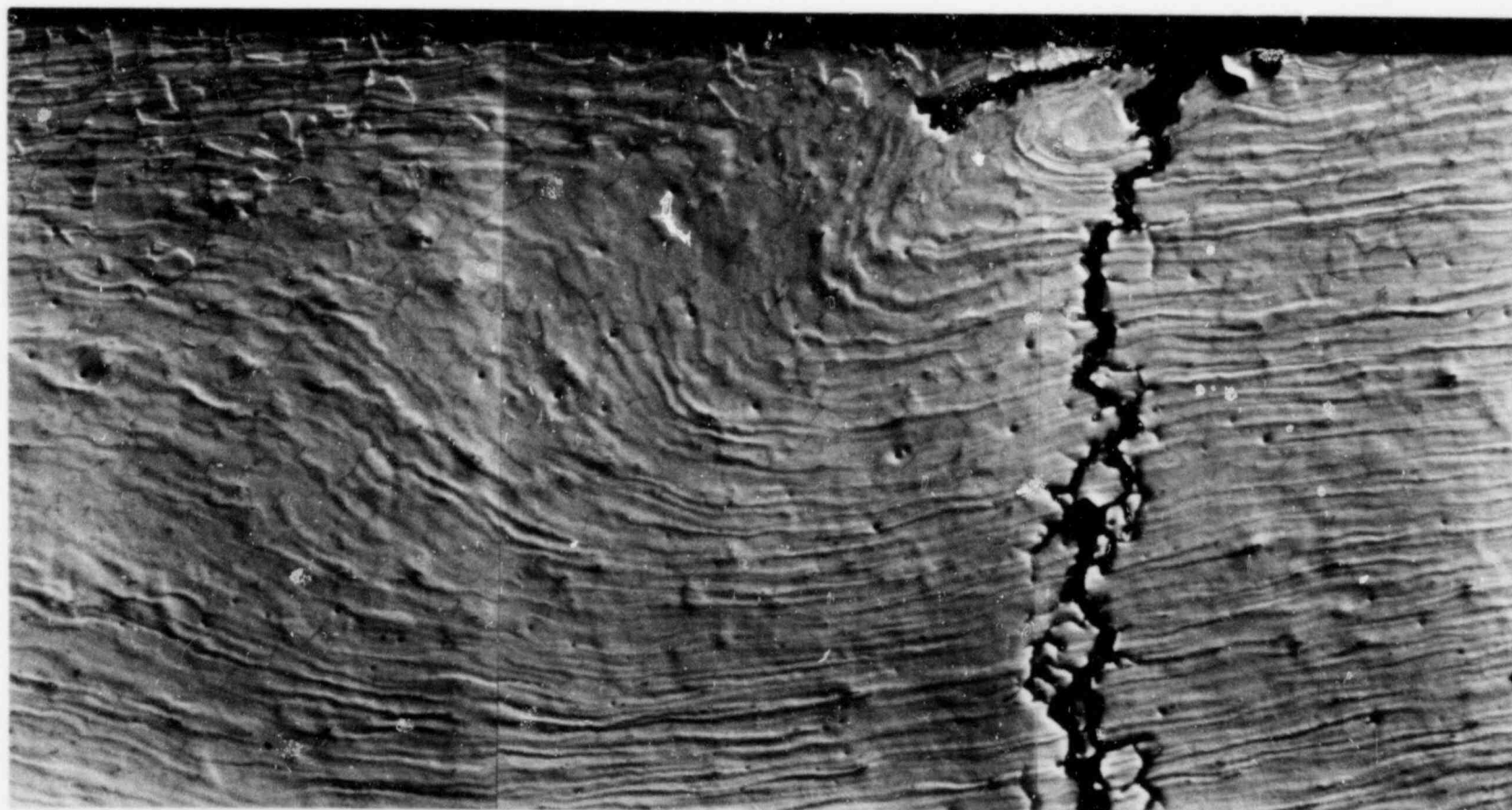
50X   Electrolytic 10% Oxalic Acid Etch   7K254

FIGURE 9.   CORING THAT REVEALS THE FLOW PATTERN OF METAL AROUND
THE LINEAR SURFACE DEFECT

The photomicrograph was taken using Nomarski
interference-contrast microscopy to enhance
the cored structure.

surface, there was a surface flaw probably introduced during the piercing
or other operation in the production of the seamless pipe. The presence
of slivers associated with other linear surface defects and the macro-
scopic appearance of most of the linear defects observed suggest that all
of the linear defects were fabrication-induced surface flaws that were
similar to laps or seams.

The crack that was associated with the surface flaw that was
examined possessed characteristics usually associated with intergranular
stress-corrosion cracking (IGSCC). The factors that led to the initiation
and propagation of IGSCC apparently were (1) the presence of the surface
flaw that acted as a stress raiser, (2) the presence of a sensitized micro-
structure in the weld heat-affected zone, (3) the corrosive environment,
that is, the water contained in the core-spray system of the reactor,
(4) the hoop tensile stress in the pipe wall as a result of the internal
pressure, and (5) possibly residual stresses in the hoop direction. In the
absence of either the surface flaw or the sensitized microstructure that
increases the susceptibility of stainless steel to IGSCC and to localized
corrosion, it is possible that IGSCC may not have occurred. The micro-
structure of the pipe in regions outside the weld heat affet zone probably
was not sensitized*, and IGSCC therefore, may not have occurred at the
linear defects located in those regions. Thus, it is advisable to examine
metallographically other defects to (1) determine the nature of the linear
defects, (2) detect the presence or absence of cracks that might be associ-
ated with the linear defects, and (3) identify the mode of crack propagation,
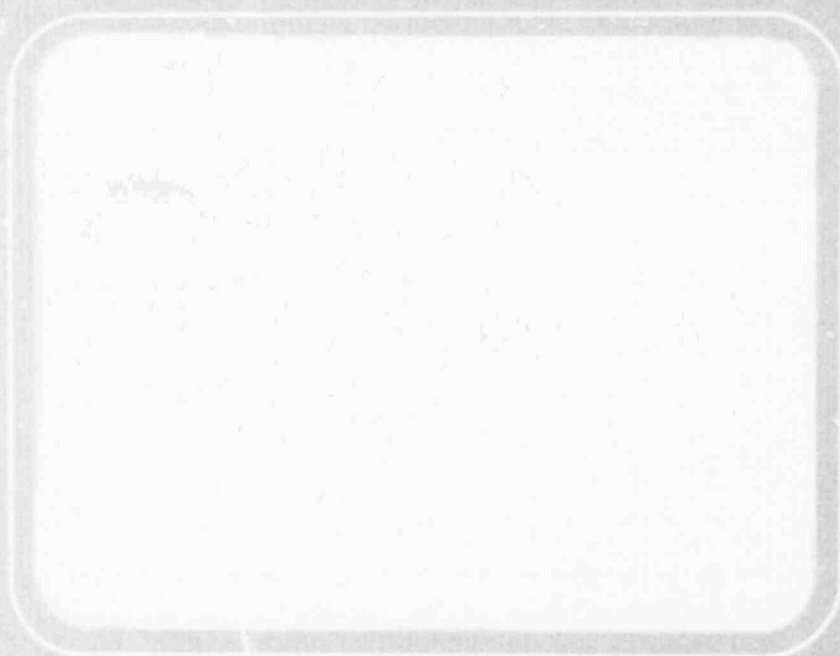if cracks are found to be present.

---

* No evidence of sensitization was found in the unaffected parent metal in
  the section shown in Figure 4.

Battelle

Columbus Laboratories

Report

FINAL REPORT

on

AN INVESTIGATION OF FLAWS ON THE
INSIDE SURFACE OF A TYPE 304 STAINLESS
STEEL SCHEDULE 80 PIPE

to

POWER AUTHORITY OF THE STATE OF NEW YORK
JAMES A. FITZPATRICK NUCLEAR POWER PLANT

July 30, 1982

by

R. D. Buchheit

BATTELLE
Columbus Laboratories
505 King Avenue
Columbus, Ohio 43201

July 30, 1982

Mr. A. V. Sorentino
Power Authority of the
    State of New York
10 Columbus Circle
New York, New York 10019

Dear Mr. Sorentino:

Enclosed are 10 copies of our final report entitled "An Investigation
of Flaws on the Inside Surface of a Type 304 Stainless Steel Schedule
80 Pipe". This report describes the details of our investigation, con-
ducted as was proposed in our letter of March 26, 1982, and the results
we obtained. The report is a sequel to our report entitled "A Metal-
lographic Investigation of a Type 304 Stainless Steel Schedule 80 Pipe",
dated March 25, 1982.

Briefly, the results of the investigation led to the basic conclusions
that (1) the flaws on the inside surface of the subject pipe were in-
duced during pipe-fabrication processing and (2) that surface flaws
located within the region of the sensitized heat-affected zone of the
circumferential weld probably served as the initiation sites of inter-
granular stress-corrosion cracking IGSCC). Surface flaws that were
located away from the weld beyond the heat-affected zone apparently did
not induce IGSCC or any other mode of failure.

The interest in this investigation was very high among all of our per-
sonnel involved in the work, and we enjoyed performing the various
tasks described in the report. If you have any questions concerning
our work or the results obtained, please feel free to contact me.

Very truly yours,

R. D. Buchheit
Physical Metallurgy Section

RDB:rw

Enc. (10)

TABLE OF CONTENTS

LIST OF TABLES

LIST OF FIGURES

LIST OF FIGURES
(Continued)

AN INVESTIGATION OF FLAWS ON THE
INSIDE SURFACE OF A TYPE 304 STAINLESS
STEEL SCHEDULE 80 PIPE

by

R. D. Buchheit

INTRODUCTION

The subject investigation is a sequel to a previous investigation
conducted by Battelle's Columbus Laboratories (BCL) of a linear defect chat
was detected on the inside surface of a pipe section using nondestructive
ultrasonic-inspection techniques. The pipe section was a section of a
12-inch-diameter Type 304 stainless steel Schedule 80 seamless pipe that
was a part of the core-spray system for a boiling-water reactor at the
James A. Fitzpatrick Nuclear Power Plant of the Power Authority of the State
of New York (PASNY). Descriptions of the details and the results of the
previous investigation are contained in the BCL report entitled " A Metal-
lographic Investigation of a Type 304 Stainess Steel Schedule 80 Pipe", dated
March 25, 1982. The summary of that report is repeated below.

> "Macroscopic examination of the inside surface of a 12-inch-
> diameter Type 304 stainess steel seamless pipe revealed the
> presence of numerous linear defects in addition to one that
> was detected by PASNY using nondestructive ultrasonic-
> inspection techniques. A cross section through one of the
> linear defects that was located close to a weld was ex-
> amined metallographically. The results of the examination
> indicated that the linear defect was most likely a
> fabrication-induced surface flaw that resembled a lap or
> seam. The surface flaw apparently acted as a stress raiser
> and, in the presence of a corrosive environment (the water
> contained in the pipe) and under the influence of hoop
> stresses induced by the internal pressure and possibly
> residual stresses in the noop direction, it led to the

initiation and propagation of an intergranular stress-corrosion crack through a sensitized region in the weld heat-affected zone."

The objectives of the subject investigation of the same section of pipe that was examined previously were (1) to examine and characterize other selected surface flaws and determine the presence or absence of cracks associated with those flaws, (2) to determine the profile of the cracks found to be present, (3) to obtain qualitative chemical analyses of corrosion products found in surface flaws and in cracks, (4) to evaluate the susceptibility of the subject pipe material to intergranular stress-corrosion cracking (IGSCC), and (5) to determine the chemical compositions of the subject pipe material and the circumferential weld metal contained in the pipe section.

The procedures used to meet the objectives of the investigation conducted by BCL and the results obtained are described in this report.

SUMMARY

Cross sections of several surface flaws were examined metallographically with the light microscope, and the susceptibility of the Type 304 stainless steel pipe to intergranular stress-corrosion cracking (IGSCC) was evaluated by electrochemical-polarization-reactivation (EPR) tests.

The cross sections through surface flaws located in the weld heat-affected zone exhibited IGSCC that had initiated and propagated from the base of those flaws. Profiles of two IGSCC's were determined from measurements of the crack depth versus crack length obtained on metallographic serial sections prepared at various intervals along the lengths of the cracks.

The cross sections through surface flaws located in regions remote from the weld heat-affected zone did not reveal the presence of IGSCC or other modes of failure associated with the surface flaws. All surface flaws exhibited characteristics of laps or seams. The appearance of the flaws and the flow patterns of metal around them indicated that the flaws were fabrication-induced during the process of forming the seamless pipe.

EPR tests indicated that the weld heat-affected zone that was sensitized was susceptible to IGSCC, whereas parent metal remote from the weld heat-affected zone was not. However, there appeared to be no IGSCC in the weld heat-affected zone in the absence of a surface flaw in that region. Hence, the surface flaws, probably acting as stress raisers, were apparently a major factor that contributed to the initiation and propagation of the IGSCC's.

Electron-microprobe analyses of corrosion products in the surface flaws and in the IGSCC's using energy-dispersive X-ray analytical techniques did not identify the corrodent(s). The corrodent was most likely the water in the core-spray system that may have contained low concentrations of oxygen and chloride that were not detected by the electron-microprobe analyses.

The chemical compositons of both the weld metal and the pipe material were found to conform to the AISI specificiations for Type 304 stainless steel.

EXPERIMENTAL PROCEDURE

The photograph in Figure 1 shows the portion of the inside surface of the Schedule 80 pipe and the surface flaws that were observed during the previous investigation. (This photograph appeared as Figure 3 in the BCL report of the previous investigation and, also, as Figure 1 in BCL's proposal for this present investigation.) The surface flaws that were selected for further studies are identified in Figure 1 by the arrows numbered 1, 2, 4 and 5. Those flaws, as numbered, conform to the manner in which those flaws were identified in BCL's proposal for this investigation. The feature identified by the arrow that was numbered 3 in that proposai is actually a part of Flaw No. 2 and is now identified as Section R-R of Flaw No. 2 in Figure 1.

Metallographic cross sections through each of the four selected flaws and perpendicular to them, as shown in Figure 1, were prepared for microscopic examinations. The resulting metallographic specimens were identified as Specimen 1-S-S for Section S-S of Flaw No. 1, Specimen 1-T-T for
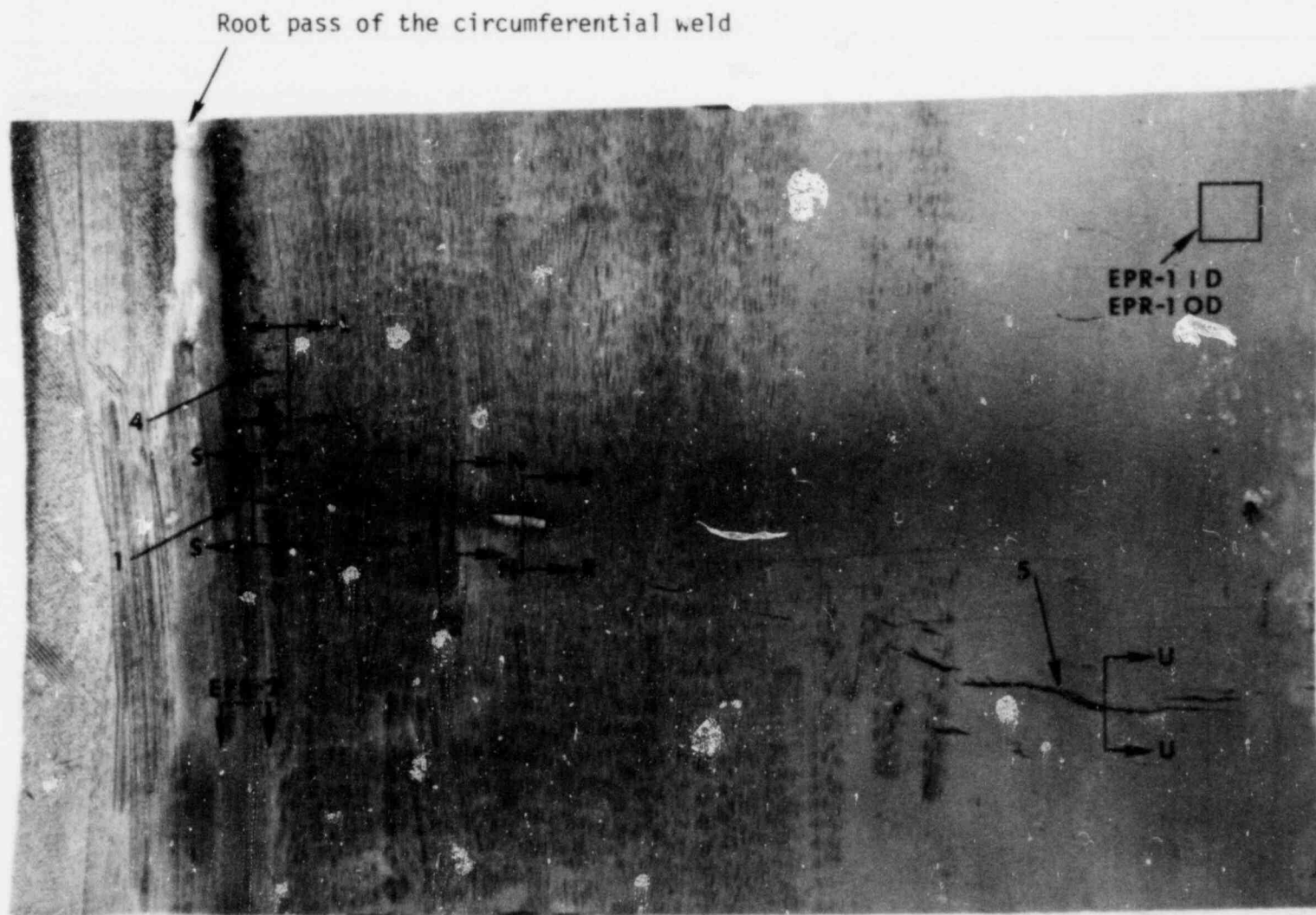
FIGURE 1. INSIDE SURFACE OF THE SCHEDULE 80 STAINLESS STEEL PIPE SHOWING SURFACE FLAWS, THE LOCATIONS OF METALLOGRAPHIC AND EPR TEST SPECIMENS, AND THE CIRCUMFERENTIAL WELD

Section T-T of Flaw No. 1, Specimen 2-P-P for Section P-P of Flaw No. 2, et cetera, for the remainder of the cross sections indicated in Figure 1.

The cross sections that revealed cracks, namely, Specimens 1-S-S, 1-T-T, 4-K-K, and 4-L-L, were successively ground, polished, and examined at measured incremental depths below each successive polished surface to establish the profiles of the cracks along the lengths of the flaws. The incremental depth measure ents served as intervals of distance along the length of the crack. At each successive plane of polish, the depth of the crack below the inside surface of the pipe and the maximum width of the crack were measured using a digital measuring microscope. Maximum crack widths always were found at or near the surface unless the crack did not penetrate the surface. The crack-depth and crack-length measurements were plotted to reveal the profile of the crack in two dimensions.

Chemical analyses of corrosion products observed in surface flaws and in cracks were obtained using energy-dispersive-X-ray (EDAX) analytical techniques in conjunction with a scanning electron microscope. Both area-scan and spot analyses were performed. The EDAX results were reported as semiquantitative analyses. The semiquantitative analysis is a standardless quantitative analysis of the X-ray-energy-spectrum data that includes a full ZAF (atomic number, absorption, and fluorescence factors) matrix-correction calculation. The relative concentrations of the elements detected are normalized to obtain a sum of 100 percent. The energy-dispersive system does not detect the lighter elements, i.e., elements of atomic number lower than 11 (sodium). Thus, for example, the concentration of oxygen that is frequently a major element in corrosion products is not included in the results of EDAX analyses.

The locations of samples used to evaluate the susceptibility of the pipe material to IGSCC are identified in Figure 1 by EPR-1 ID, EPR-1 OD, and EPR-2. The evaluation was accomplished by performing electrochemical-polarization-reactivation (EPR) tests of the inside and outside pipe surfaces some distance from the weld and of a region of the weld heat-affected zone. A through-wall piece of the pipe approximately 1/2 inch square was sectioned in half at the midwall to provide Sample EPR-1 ID for the inside pipe sur-face and Sample EPR-1 OD for the outside pipe surface. Those surfaces were

ground slightly and polished to provide suitable flat surfaces for the EPR tests. A polished cross section of the weld heat-affected zone was obtained to provide Sample EPR-2. Since experience has shown that the presence of weld metal in the test sample interferes with the results of the EPR test, all of the weld metal in Sample EPR-2 was ground away.

Quantitative chemical analyses of the pipe material and the weld metal were obtained using emission-spectographic analytical techniques. The analysis of the pipe material was determined on the surface of a through-wall section of the pipe that was obtained from a location adjacent to the location of the EPR-1 ID and EOR-1 OD samples. The analysis of the weld metal was determined on the surface of a through-wall section of the pipe along the center line of the weld; that section of the weld was obtained from a location that was adjacent to the location of the EPR-2 sample.

EXAMINATIONS AND RESULTS

Chemical Analyses

The chemical compositions of the Type 304 stainless steel Schedule 80 pipe and the circumferential weld metal that joined the straight-pipe section to an elbow section are presented in Table 1. The specified composition of AISI Type 304 stainless steel is included in Table 1 for comparison. The chemical compositions of both the pipe and the weld metal were found to conform to the AISI specifications for Type 304 stainless steel.

Crack-Profile Determinations

Flaw No. 1 in Figure 1

The metallographic examination of Specimen 1-S-S (see Figure 1) during the previous investigation of the Schedule 80 pipe revealed the presence of IGSCC extending from the bottom of Flaw No. 1 at the inside pipe surface toward the outside surface through about 77 percent of the wall thickness. In the present investigation, the profile of that crack along

TABLE 1.   RESULTS OF EMISSION-SPECTROGRAPHIC ANALYSES OF THE TYPE 304
            STAINLESS STEEL PIPE AND THE STAINLESS STEEL WELD METAL OF
            THE CIRCUMFERENTIAL WELD

| Element | Content, weight percent | | |
	Pipe	AISI Type 304 Specifications	Weld Metal
Carbon	0.045	0.08 max	0.032
Manganese	1.73	2.0 max	1.42
Phosphorus	0.021	0.045 max	0.014
Sulfur	0.016	0.030 max	0.007
Silicon	0.65	1.0 max	0.63
Nickel	10.3	8-10.5	9.6
Chromium	18.3	18-20	19.1
Molybdenum	0.18		0.10
Vanadium	0.05		0.05
Aluminum	0.007		0.042
Copper	0.10		0.065
Tin	0.008		0.006
Columbium	0.008		0.011
Zirconium	0.005		0.006
Titanium	0.004		0.006
Boron	0.0005		0.0007
Cobalt	0.11		0.10
Tungsten	0.00		0.00
Iron	68.73		68.78

its length was obtained from serial sections of Specimen 1-S-S and Specimen 1-T-T; the profile is revealed in Figure 2 by a plot of the depths of the crack below the inside pipe surface at various intervals of distance along the length of the crack. Zero distance in Figure 2 corresponds to the location (termed a reference plane) where no crack was observed beyond the end of the flaw next to the weld metal; in this case, the reference plane was entirely within the weld metal. The abscissa in Figure 2 extends away from the weld through its heat-affected zone and in a direction along the length of the flaw. The crack-depth and crack-length data that are plotted in Figure 2 are given in Table 2.

The cross-hatched region in Figure 2 represents the extent of the IGSCC surface. Included in Figure 2 are the approximate locations of the inside and outside pipe surfaces and portions of the weld line with respect to the crack. Note that IGSCC penetrated weld metal where crack propagation eventually arrested. However, crack propagation extended a short distance beyond the final pass of weld metal on the outside pipe surface and, in fact, reached the outside surface in one small region. It is interesting to note here that no leakage of the core-spray pipe system was reported.

Figure 3 shows the appearance of the IGSCC at a few locations along its length. Figure 3a exhibits the crack at the 0.060-inch position. At that location the crack was subsurface and entirely within weld metal. At the 0.290-inch position, Figure 3b, the crack extended through approximately 77 percent of the pipe wall. Figure 3c exhibits the portion of the crack near the outside surface of the pipe at the 0.702-inch position (at much higher magnification); essentially the entire crack in the through-wall direction is shown.

The appearance of the surface flaw at the 0.70-inch position is revealed in Figure 4. The flaw exhibited two surface imperfections that were approximately 0.1 inch apart; those two inperfections are shown in Figures 4a and 4b respectively. A little IGSCC was still evident at the flaw shown in Figure 4b.

The flow pattern of the metal that developed around the flaw during the fabrication of the pipe was revealed by etching metallographically polished specimens, as is shown in Figure 5 at a magnification of 50X. At

Weld metal →

ID surface

Nominal pipe-wall thickness

Estimate of weld line

Distance Below Inside Pipe Surface, inches

OD surface

Weld metal →
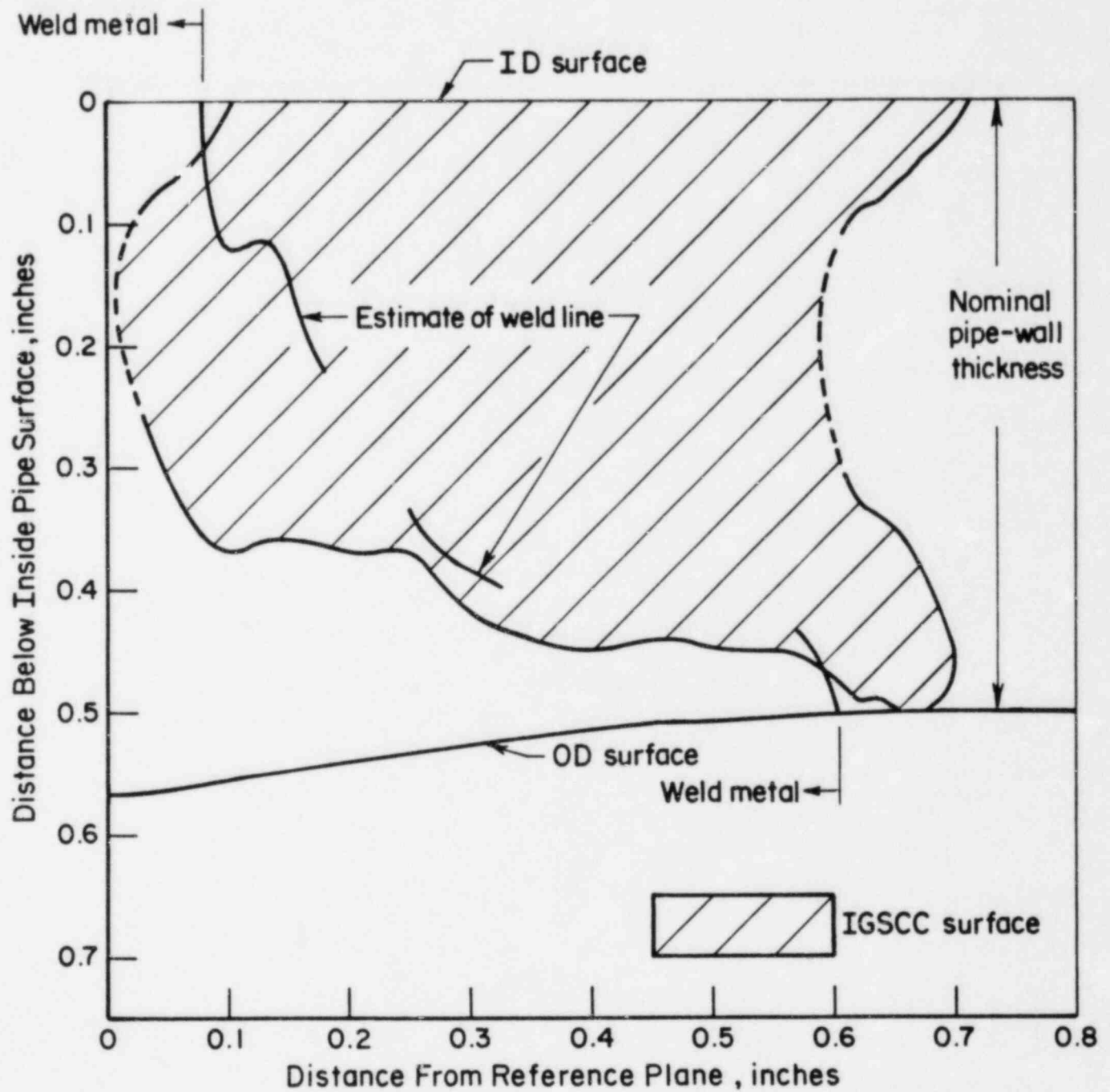
IGSCC surface

Distance From Reference Plane, inches

FIGURE 2. PROFILE OF INTERGRANULAR STRESS-CORROSION CRACK
AT FLAW NO. 1

TABLE 2. CRACK-DEPTH AND CRACK-LENGTH DATA FOR THE IGSCC
ASSOCIATED WITH FLAW NO. 1

Specimen of Flaw No. 1	Distance from Reference Plane,[a] inches	Depth of Crack Below Inside Pipe Surface, inches	Maximum Width of Crack, mils
1-S-S	0	No crack	-
	0.030	0.092 to 0.255	0.4
	0.060	0.059 to 0.328	0.7
	0.100	0.008 to 0.373	1.0
(Surface Flaw No. 1 begins)	?		
	0.130	0.357	1.0
	0.170	0.364	1.4
	0.210	0.366	1.4
	0.250	0.366	1.7
	0.290	0.410	2.0
1-T-T	0.322	0.429	2.0
	0.362	0.443	3.0
	0.412	0.448	1.0
	0.462	0.443	2.0
	0.512	0.447	2.0
	0.562	0.449	2.0
(Weld Metal at OD ends)	?		
	0.612	0.108 and 0.305 to 0.482	0.8 and 0.6
	0.622	0.087 and 0.326 to 0.487	0.5 and 0.4
	0.637	0.083 and 0.337 to 0.492	0.8 and 0.4
	0.652	0.069 and 0.349 to 0.497	0.9 and 0.3
	0.677	0.043 and 0.391 to 0.496	0.7 and 0.3
	0.702	0.019 and 0.452 to 0.470	0.4 and 0.1
(Flaw No. 1 ends)	?		
	0.717	No crack	-

(a) The distance from a reference plane of polish just beyond the end of the crack that was in the weld.

FIGURE 3. THE IGSCC ASSOCIATED WITH FLAW NO. 1 AT SEVERAL LOCATIONS ALONG THE LENGTH OF THE CRACK

100X   7K993
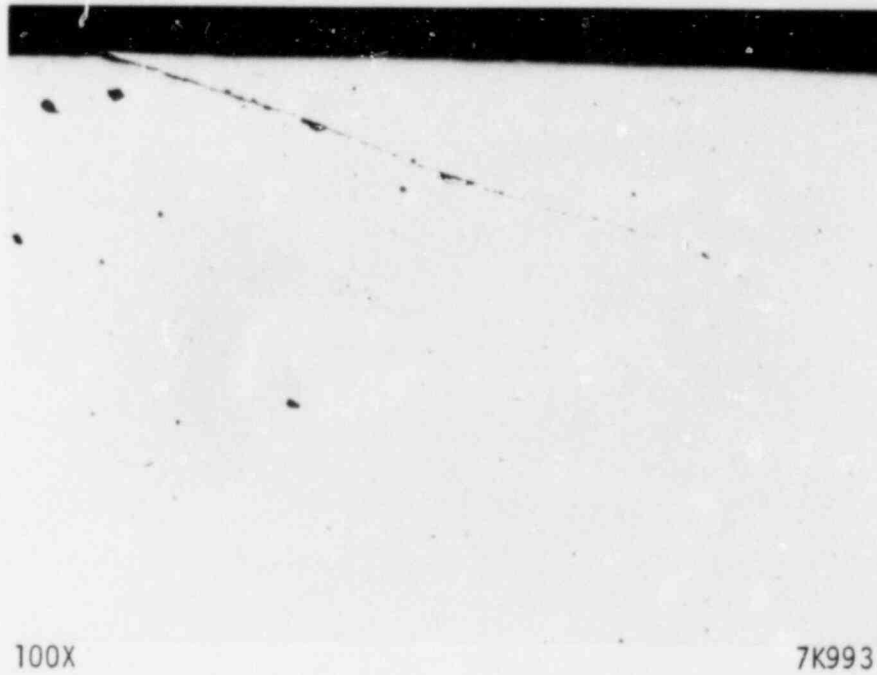
a. Surface Imperfection Located About 0.1 Inch from the Imperfection Shown in (b) Below

100X   7K992
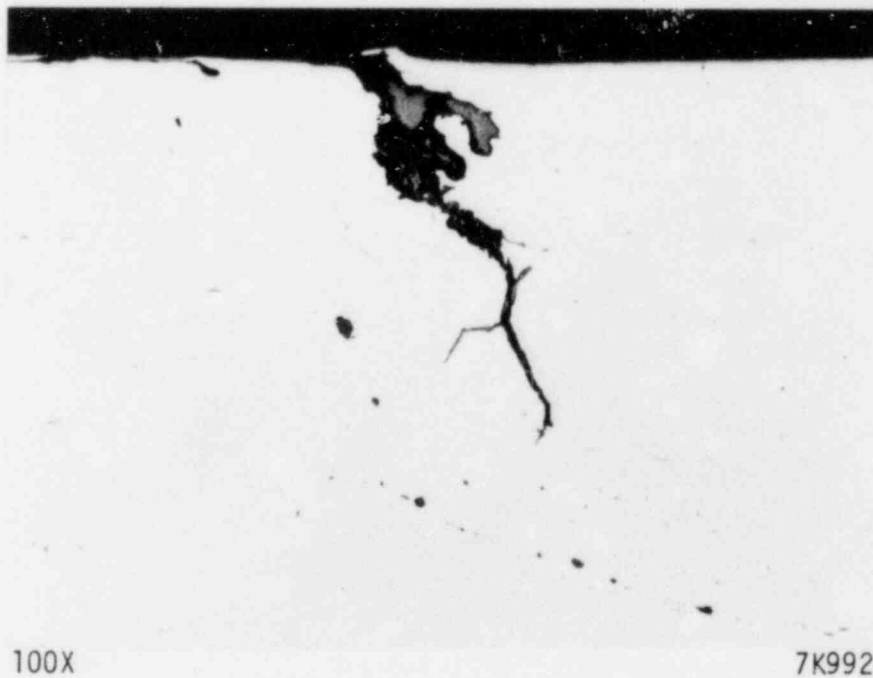
b. Surface Imperfection and Some IGSCC at the 0.70-Inch Position

FIGURE 4. FLAW NO. 1 NEAR THE END OF THE IGSCC FARTHEST FROM THE WELD

50 X

8K018

Glyceregia Etch

FIGURE 5. THE FLOW PATTERN OF METAL AROUND FLAW NO. 1 AT THE 0.72-INCH LOCATION IN FIGURE 2

The photomicrograph was taken using Nomarski interference-contrast microscopy to enhance the metal-flow pattern.

that magnification, the two surface imperfections shown in Figure 4a and 4b are evident. The cross section of the flaw in Figure 5 is located at approximately the 0.72-inch position in Figure 2; that cross section is about 0.02 inch beyond the cross section shown in Figure 4. In Figure 5, the surface imperfection shown in Figure 4a is observed to be slightly larger, and the surface imperfection shown in Figure 4b is observed to be slightly smaller with little or no evidence of IGSCC,

Flaw No. 4 in Figure 1

Flaw No. 4, like Flaw No. 1, was located in close proximity to the weld in the region of the weld heat-affected zone. At that location, the propagation of IGSCC from the flaw was suspected and was observed in metallographic cross sections of the flaw. The profile of the crack was obtained from serial sections of Specimen 4-K-K and Specimen 4-L-L. When Specimen 4-K-K was prepared metallographically, it was anticipated that no crack would be present in the initial section, because the section was obtained beyond the end of the flaw that was visible on the surface of the pipe. However, a crack was present; therefore Specimen 4-L-L was prepared in order to determine the extent of the crack in a direction away from the weld. The profile of the IGSCC crack at Flaw No. 4 is revealed in Figure 6 in the same manner as was the crack-profile presented in Figure 2. The data for crack depth and crack length that are plotted in Figure 6 are given in Table 3.

The cross-hatched region in Figure 6 represents the extent of the IGSCC surface. Included in Figure 6 are the approximate locations of the inside and outside pipe surfaces and a portion of the weld line, with respect to the crack. Although the crack-surface area was smaller, the general outline of that area was similar to that of the IGSCC at Flaw No. 1 (compare Figures 2 and 6). Also, arrest of the crack propagation in the through-wall direction again apparently occurred in weld metal.

Figure 7 shows the appearance of the IGSCC at a few locations along its length. Figure 7a exhibits the crack at the 0.10-inch position. At that location, the crack was subsurface and was entirely within weld metal except for a very small portion near middepth. At the 0.125-inch position (Figure 7b), the crack was slightly beneath the inside surface of the pipe and had begun to
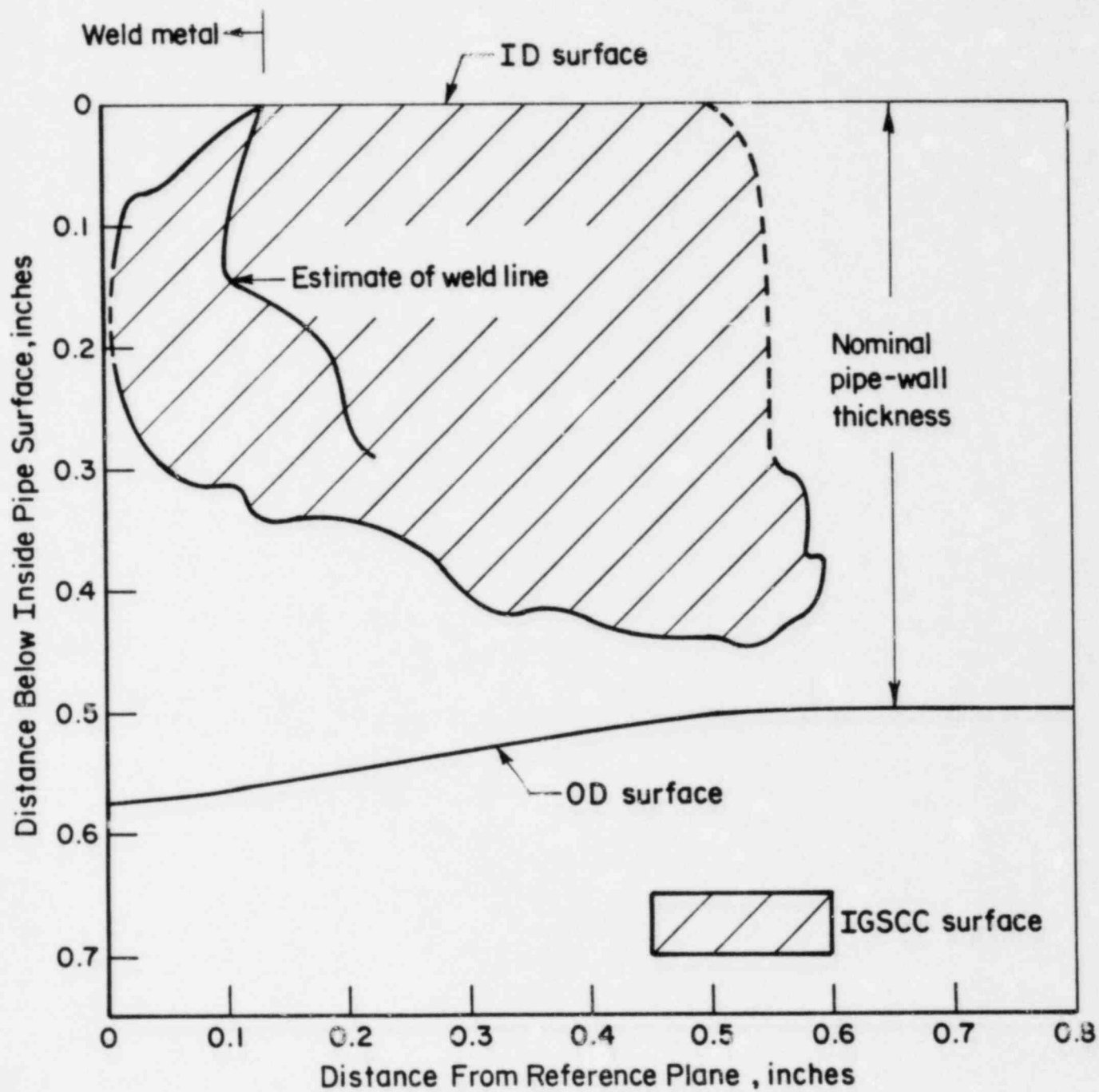
FIGURE 6.   PROFILE OF INTERGRANULAR STRESS-CORROSION CRACK AT FLAW NO. 4

TABLE 3. CRACK-DEPTH AND CRACK-LENGTH DATA FOR THE IGSCC
ASSOCIATED WITH FLAW NO. 4

Specimen of Flaw No. 4	Distance from Reference Plane,[a] inches	Depth of Crack Below Inside Pipe Surface, inches	Maximum Width of Crack, mils
4-K-K	0	No crack	-
	0.010	0.133 to 0.213	0.2
	0.022	0.06i to 0.256	0.5
	0.047	0.069 to 0.296	1.0
	0.097	0.023 to 0.315	1.0
	0.112	0.014 to 0.315	1.0
	0.127	0.004 to 0.341	1.0
	0.142	0.345	1.2
	0.161	0.340	1.2
	0.187	0.338	1.8
	0.212	0.346	1.3
	0.262	0.367	1.6
	0.312	0.415	1.0
	0.372	0.415	1.5
	0.431	0.437	1.0
	0.491	0.441	0.6
	0.511	0.008 to 0.441	0.5
	0.517	0.012 to 0.444	0.5
4-L-L	0.554	0.295 to 0.438	0.3
	0.559	0.299 to 0.437	0.2
	0.565	0.305 to 0.431	0.15
	0.575	0.313 to 0.425	0.15
	0.585	0.373 to 0.415	0.1
	0.597	0.376 to 0.385	0.05
	0.607	No crack	-

(a) The distance from a reference plane of polish just beyond the end of the crack that was in the weld.
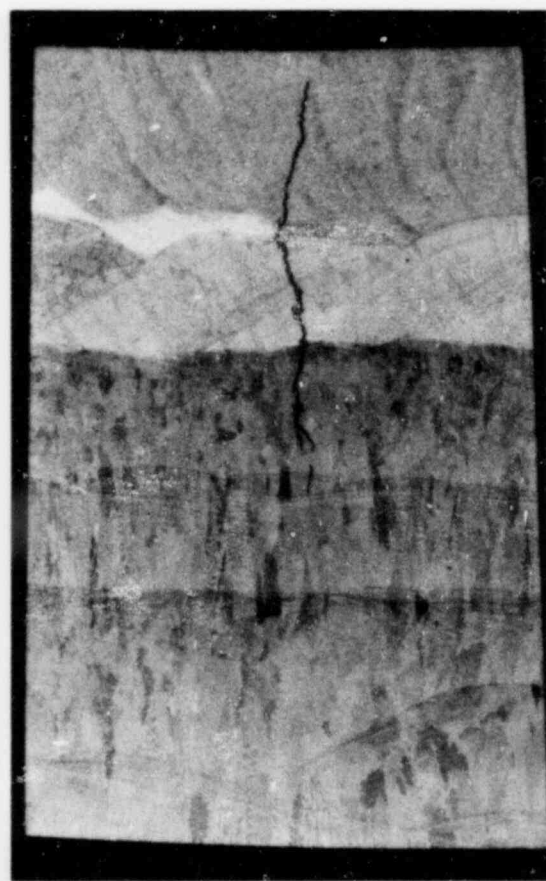
| 7X | Glyceregia Etch | 8K001 | 7X | Glyceregia Etch | 8K000 | 7X | Glyceregia Etch | 7K999 |

a. IGSCC at the 0.10-Inch Position   b. IGSCC at the 0.125-Inch Position   c. IGSCC at the 0.161 Inch Position
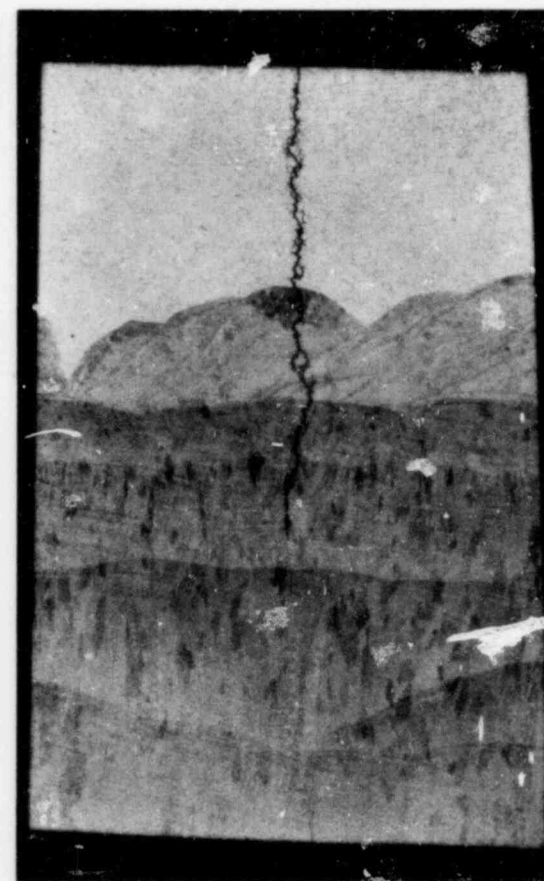
FIGURE 7.   THE IGSCC ASSOCIATED WITH FLAW NO. 4 AT SEVERAL LOCATIONS ALONG THE LENGTH OF THE CRACK

17

7X   As Polished   7K998   500X   As Polished   7K997

     d.   IGSCC at the 0.517-
        Inc' Position

                                     e.   IGSCC at the 0.597-
                                          Inch Position

FIGURE 7.   (Continued)

penetrate the root pass of the weld.   Figure 7c shows the crack at the 0.161-inch position.

The first plane of polish in Specimen 4-K-K revealed the IGSCC as shown in Figure 7d. As was mentioned earlier, the presence of a crack in this plane of polish was not anticipated, because Specimen 4-K-K was beyond the visible end of Flaw No. 4. Not only was the crack present, but the depth of the crack was nearly a maximum and a second, adjacent crack was observed. The second crack is evident in Figure 7d to the left of the primary crack. In this section, both the primary crack and the secondary crack began below the inside surface of the pipe. Neglecting the distance between the pipe surface and the beginning of the crack below the pipe surface, the primary crack extended in depth about 89 percent of the pipe-wall thickness. The secondary crack was not plotted in Figure 6, because its presence was observed only between the 0.49- and 0.52-inch locations and it did not extend beyond a depth below the pipe surface of about 0.12 inch. The secondary crack may have been a branch of the primary crack.

Figure 7e exhibits the IGSCC crack near the outside suface of the pipe at about the 0.60-inch position at high magnification; the entire crack in the through-wall direction is shown. No crack was observed in the next serial section beyond 0.60 inch.

Examinations of Other Surface Flaws

The examinations of cross sections of other surface flaws, namely Specimens 2-P-P, 2-N-N, 2-R-R, and 5-U-U (see Figure 1), did not reveal the presence of IGSCC nor any other mode of failure induced by the surface flaws. All of the surface flaws examined exhibited characteristics similar to those generally observed for seams or laps in billet surfaces. Examples of those characteristics are shown in Figures 8 through 11. The three cross sections of Flaw No. 2 are presented in Figures 8 through 10. In Specimen 2-P-P in Figure 8, the depth of Flaw No. 2 was observed to be relatively shallow. The slight depression in the surface of the pipe, indicated by the arrow in Figure 8, and the curved flow pattern of metal below that depression suggest that a thin, sliver of surface metal may have been present at that location

Possible site of a thin sliver of surface metal

50X

Glyceregia Etch

8K020

FIGURE 8. THE FLOW PATTERN OF METAL AROUND SURFACE FLAW NO. 2 OBSERVED IN SPECIMEN 2-P-F

The photomicrograph was taken using Nomarski interference-contrast microscopy to enhance the metal-flow pattern.

8K019

50X

Glyceregia Etch

FIGURE 9.   THE FLOW PATTERN OF METAL AROUND SURFACE FLAW NO. 2 IN SPECIMEN 2-N-N

The photomicrograph was taken using Normarski inteference-contrast microscopy to enhance the metal-flow pattern.

50X Glyceregia Etch 8K021

FIGURE 10. THE FLOW PATTERN OF METAL AROUND SURFACE FLAW NO. 2 IN SPECIMEN 2-R-R

The photomicrograph was taken using Nomarksi interference-contrast microscopy to enhance the metal-flow pattern.
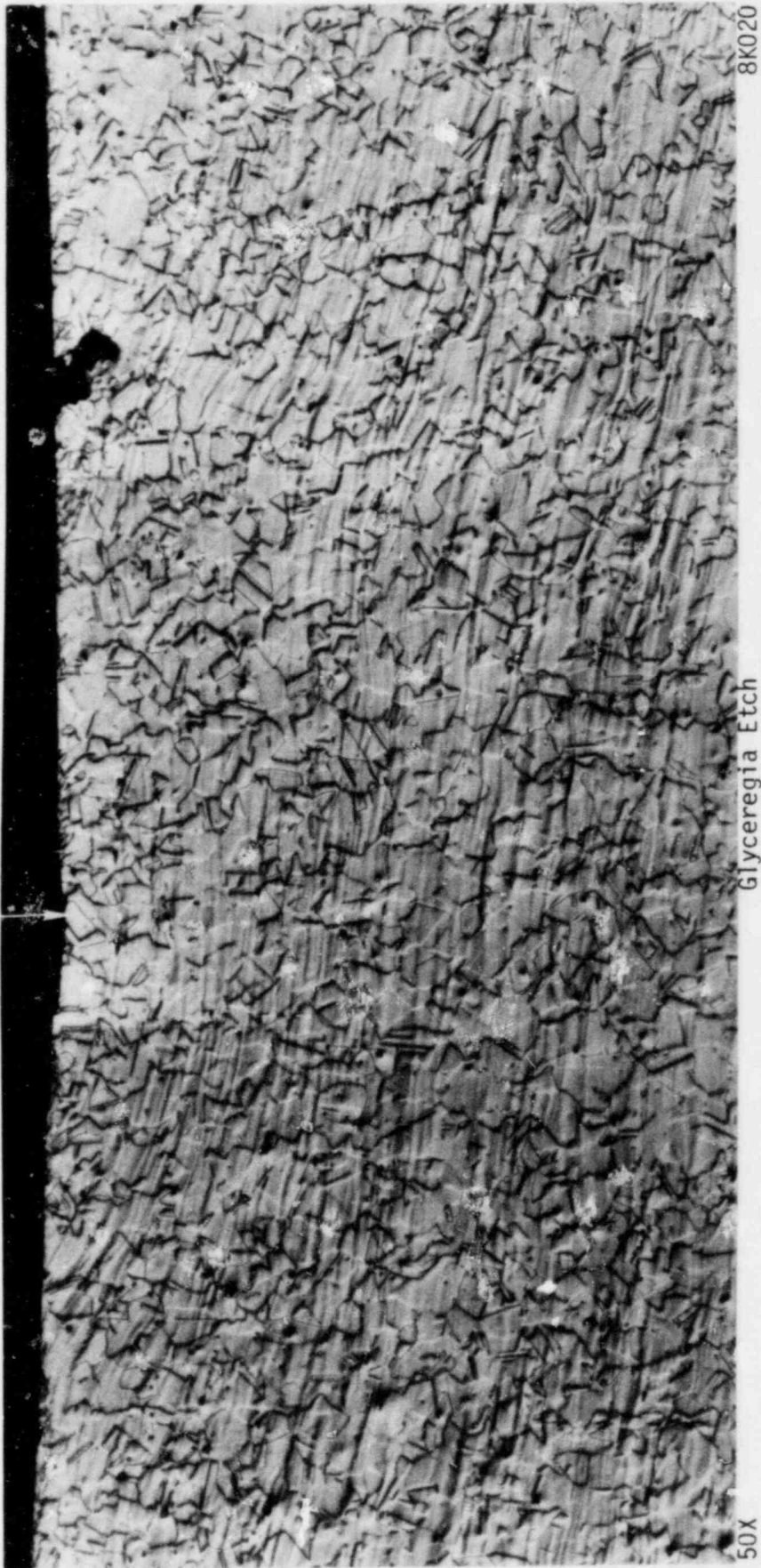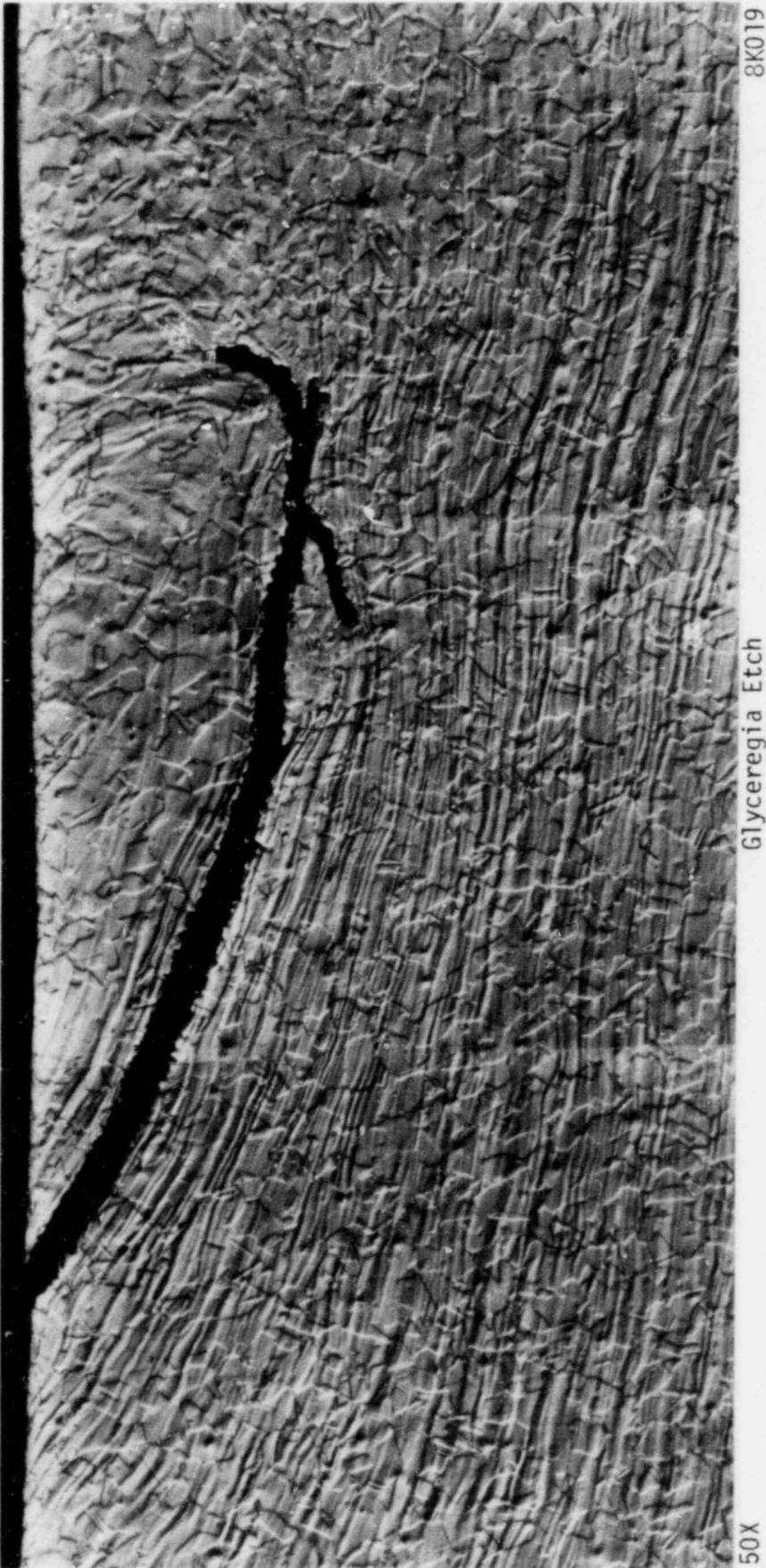
22

50X Glyceregia Etch 8K022

FIGURE 11. THE FLOW PATTERN OF METAL AROUND SURFACE FLAW NO. 5 IN SPECIMEN 5-U-U

The photomicrograph was taken using Nomarski interference-contrast microscopy to enhance the metal-flow pattern.

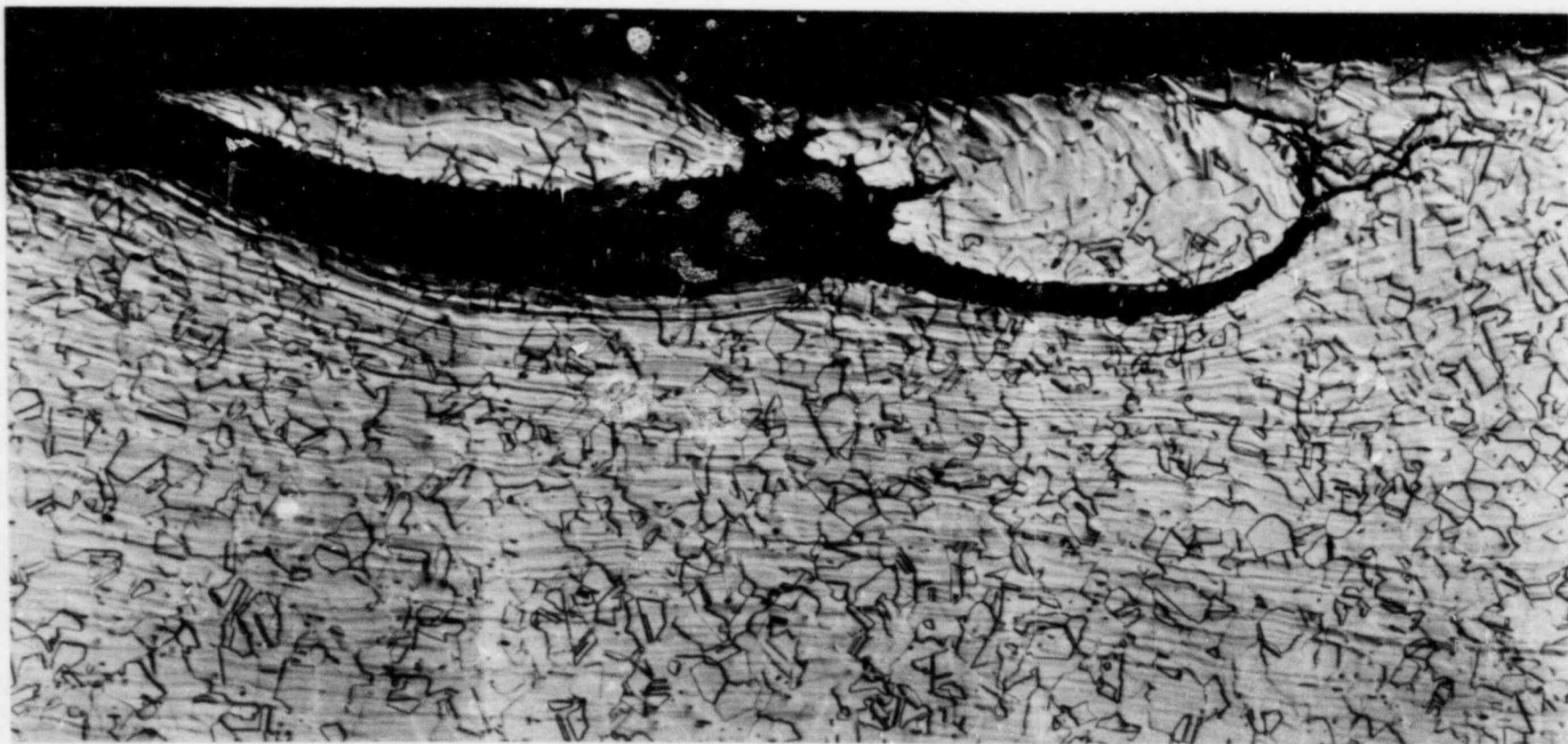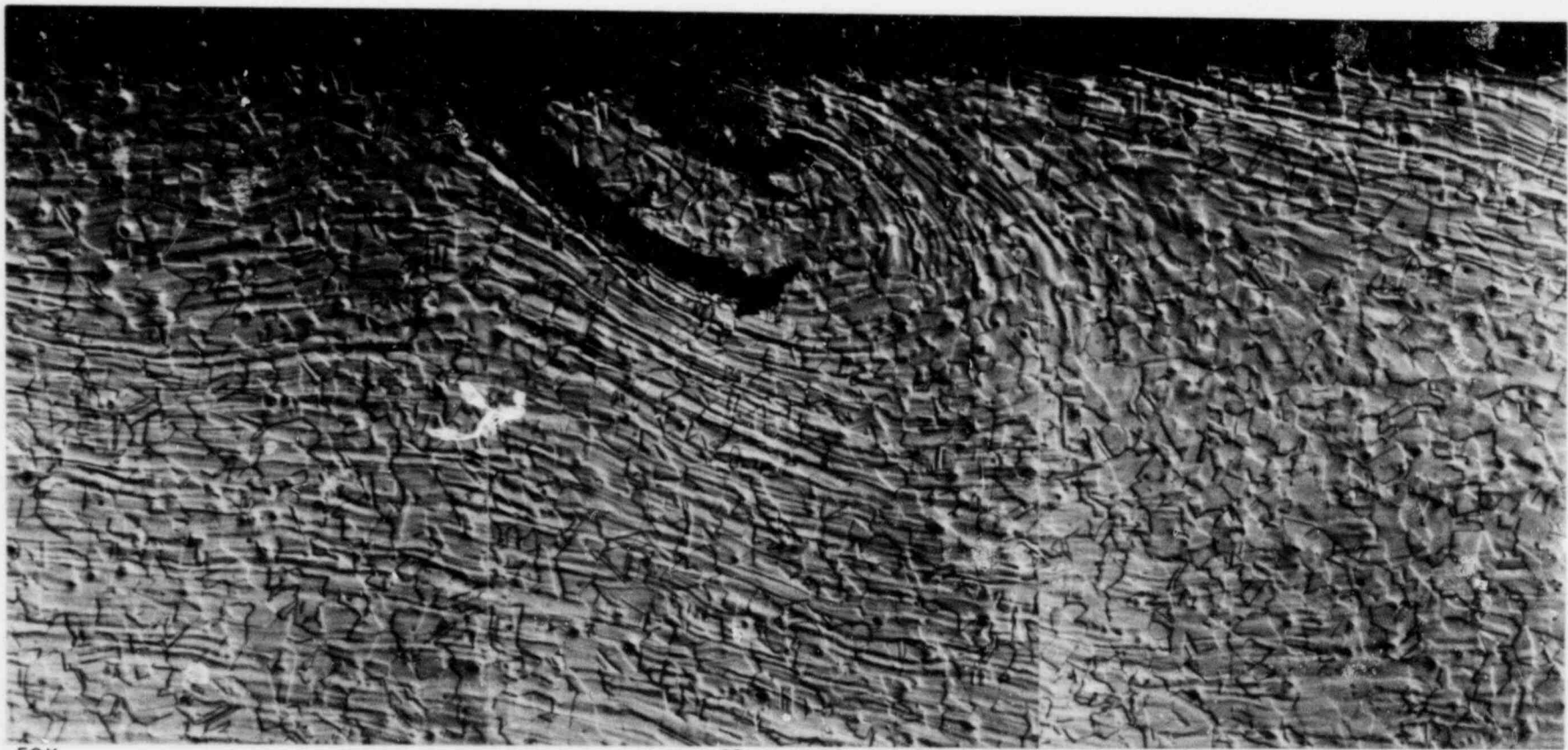at some earlier time. Specimen 2-N-N was taken at approximately the mid-
length of Flaw No. 2. In that section, shown in Figure 9, the flaw appears
very much like a surface fold, or lap. The depth of the flaw was about
0.035 inch. Specimen 2-R-R was taken across a thin sliver of surface metal
that had been lifted, but not removed, from the surface; the appearance of
the sliver can be seen in Figure 10. Part of the sliver was detached from
the surface of the pipe at the location of Specimen 2-R-R.

Specimen 5-U-U across Flaw No. 5 is shown in Figure 11. The
characteristics of Flaw No. 5 were similar to those of Flaw No. 2 (and Flaw
No. 1 that was presented earlier in this report and in the report of the
previous investigation). The depth of Flaw No. 5 was about 0.030 inch.

The flow patterns of metal that were revealed around the flaws
indicated that the surface flaws developed during the fabrication of the
seamless pipe; hence, the flaws were present in the pipe when the pipe was
installed in the core-spray piping system.

Energy-Dispersive X-ray Analyses

Chemical analyses of the corrosion products observed in Flaw No. 1
and the IGSCC associated with that flaw were made in Specimen 1-S-S before
the serial sections were prepared. Analyses of the corrosion products in
other surface flaws were made in Specimens 2-N-N and 2-R-R of Flaw No. 2
and in Specimen 5-U-U of Flaw No. 5.

Corrosion Products in Flaw No. 1

The results of the semiquantitative energy-dispersive X-ray (EDAX)
electron-microprobe analyses of corrosion products observed within Flaw
No. 1 in the IGSCC associated with the flaw are presented in Table 4. The
results of EDAX analyses of the AISI 304 stainless steel pipe and the weld
metal in Specimen 1-S-S are included in Table 4 as base data for comparison
with the results obtained from the analyses of the corrosion products.

TABLE 4. RESULTS OF SEMIQUANTITATIVE[a] ELECTRON-MICROPROBE
ANALYSES OF CORROSION PRODUCTS BY ENERGY-DISPERSIVE-
X-RAY ANALYTICAL TECHNIQUES IN SPECIMEN 1-S-S
OF FLAW NO. 1

	Area Analyzed	Relative Concentration of the Elements Detected[b], percent			
		Fe	Cr	Ni	Si
1	304 SS matrix	69.6	18.9	10.4	1.0
2	304 SS weld metal	69.4	19.7	9.8	1.1
3	Corrosion products in Flaw No. 1 (see Figure 13)	56.4	36.1	6.3	1.2
4	Corrosion products in the main crack near the inside pipe surface (see Figure 15)	93.9	0.9	5.3	ND[c]
5	Corrosion products in a branch crack	69.0	24.2	5.9	0.9
6	Corrosion products in a branch crack near Area 5	47.9	44.0	6.5	1.5
7	Corrosion products in the main crack at about middepth	93.3	1.3	5.3	ND
8	Corrosion products in the main crack near the crack tip in the weld metal	92.1	2.9	5.0	ND

(a) The semiquantitative analysis is a standardless quantitative analysis of the X-ray-energy-spectra data that includes a full ZAF (atomic number, absorption, and fluorescence factors) matrix-correction calculation. The relative concentrations of the elements detected are normalized to obtain a sum of 1.0 (100 percent).

(b) Elements lighter than Atomic Number 11 (sodium) are not detected, so oxygen could not be determined.

(c) ND = not detected.

The relative concentrations of chromium and nickel in the pipe (Area 1 in Table 4) and in the weld metal (Area 2 in Table 4) agree quite well with the contents of those two elements that were obtained by emission-spectrographic analytical techniques. (Refer to Table 1 for the comparison.) The X-ray-energy spectrum for the pipe, which was nearly the same as the spectrum for the weld metal, is shown in Figure 12.

The corrosion products that were analyzed in Flaw No. 1 (Area 3 in Table 4) are identified by the arrow in Figure 13, a cross section of Flaw No. 1 observed in Specimen 1-S-S. The X-ray-energy spectrum for Area 3 is presented in Figure 14. The analysis of the chromium present in the corrosion products indicated that the chromium content was nearly twice the chromium content of the pipe. The increase in the chromium content was accompanied by decreases in the iron and nickel contents.

The region represented by Area 4 in Table 4, a region of corrosion products in the IGSCC below Flaw No. 1 near the inside surface of the pipe, is shown in Figure 15a. Those corrosion products contained a relatively low concentration of chromium, as was indicated also by the X-ray-energy spectrum of Area 4 presented in Figure 16. The X-ray distribution map of chromium presented in Figure 15b indicates the low concentration of chromium in the major portion of the corrosion products in the grain boundaries. (A region that exhibits a relatively sparse population of white dots in an X-ray-distribution map of an element indicates that the region contains a lower concentration of the element than do the regions that exhibit more dense populations of white dots.) The major decrease in the chromium content was balanced by a major increase in the iron content.

Areas 5 and 6 in Table 4 were the regions of corrosion products observed in two different, but nearby, intergranular cracks that branched out from the main intergranular crack. The chromium and iron contents appeared to differ significantly between those two areas, and the chromium content in both areas was well above that in the pipe. The X-ray-energy spectrum of Area 6 is shown in Figure 17.

The analyses of corrosion products in the main crack at about middepth below the inside pipe surface and of corrosion products near the crack tip in the weld metal both exhibited relatively low concentrations of

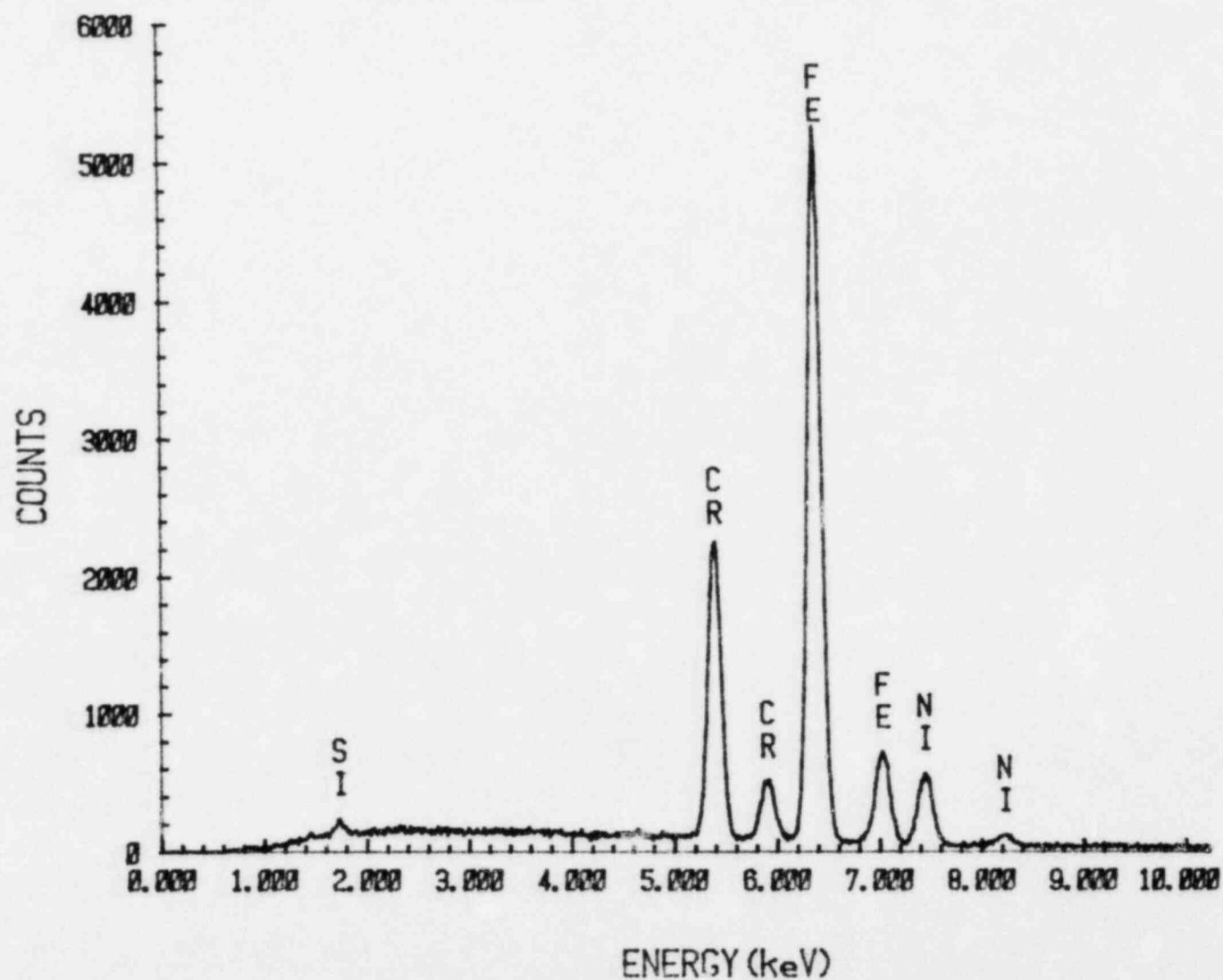FIGURE 12.   ENERGY-DISPERSIVE X-RAY SPECTRUM OBTAINED FROM AN ANALYSIS OF THE TYPE 304
STAINLESS STEEL MATRIX IN SPECIMEN 1-S-S OF FLAW NO. 1 (AREA 1 in TABLE 4)

100X   As Polished   7K243

FIGURE 13.   CROSS SECTION OF FLAW NO. 1 IN SECTION 1-S-S

The arrow identifies the corrosion products
in Flaw No. 1 (Area 3 in Table 4) that were
subjected to EDAX analyses.

FIGURE 14. ENERGY-DISPERSIVE X-RAY SPECTRUM OBTAINED FROM AN ANALYSIS OF CORROSION
PRODUCTS IN FLAW NO. 1 OBSERVED IN SPECIMEN 1-S-S (AREA 3 in TABLE 4)

1000X   34692
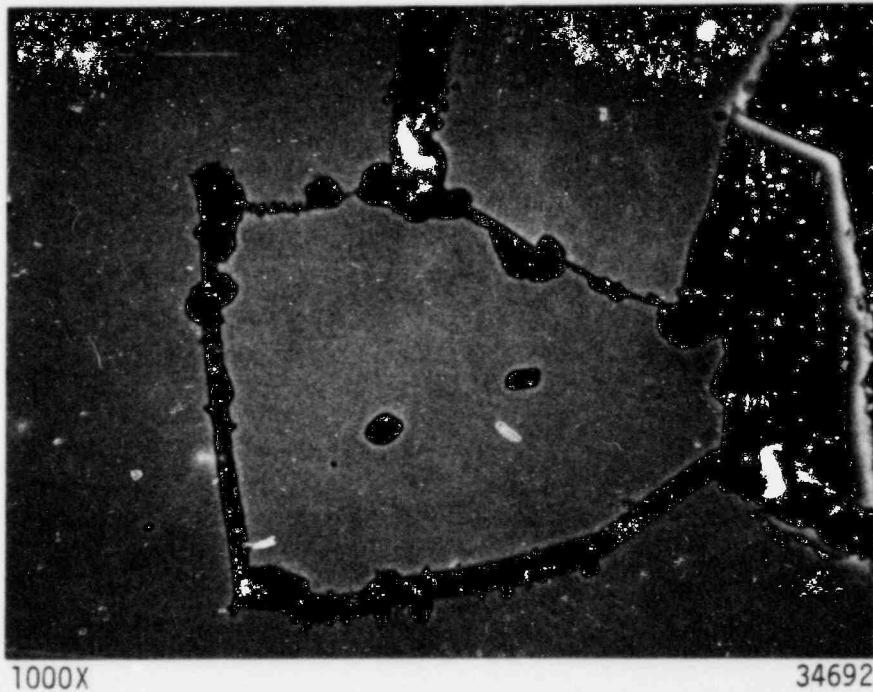
a. Region of the IGSCC Identified As
   Area 4 in Table 4 (SEM Micrograph)

1000X   34693

b. X-ray-Distribution Map of Cr in the
   Region Shown in (a) Above

FIGURE 15. CORROSION PRODUCTS IN THE IGSCC NEAR THE
            INSIDE SURFACE OF THE PIPE

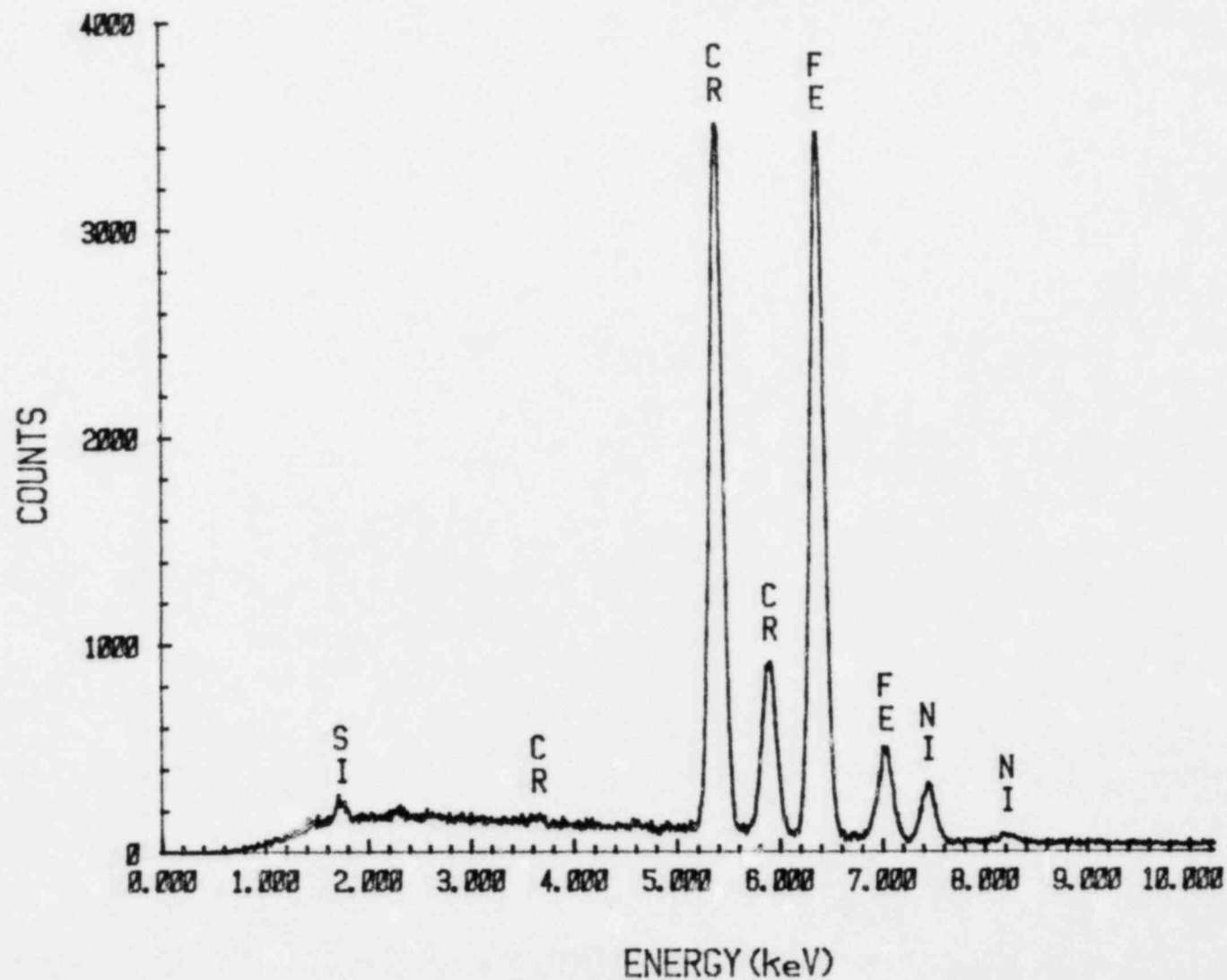FIGURE 16.   ENERGY-DISPERSIVE X-RAY SPECTRUM OBTAINED FROM AN ANALYSIS OF CORROSION PRODUCTS
IN THE CRACK (AREA 4 IN TABLE 4)
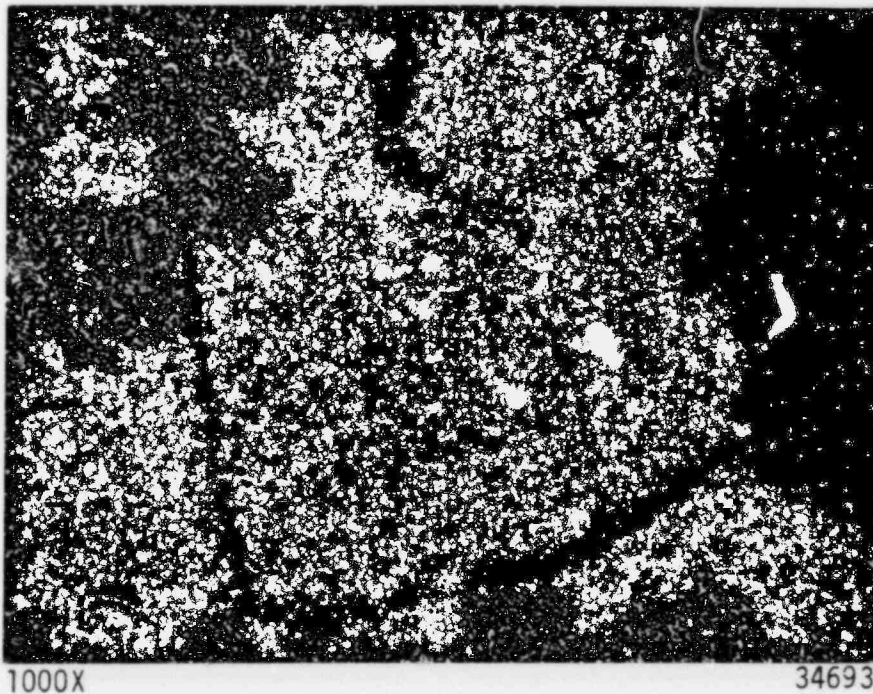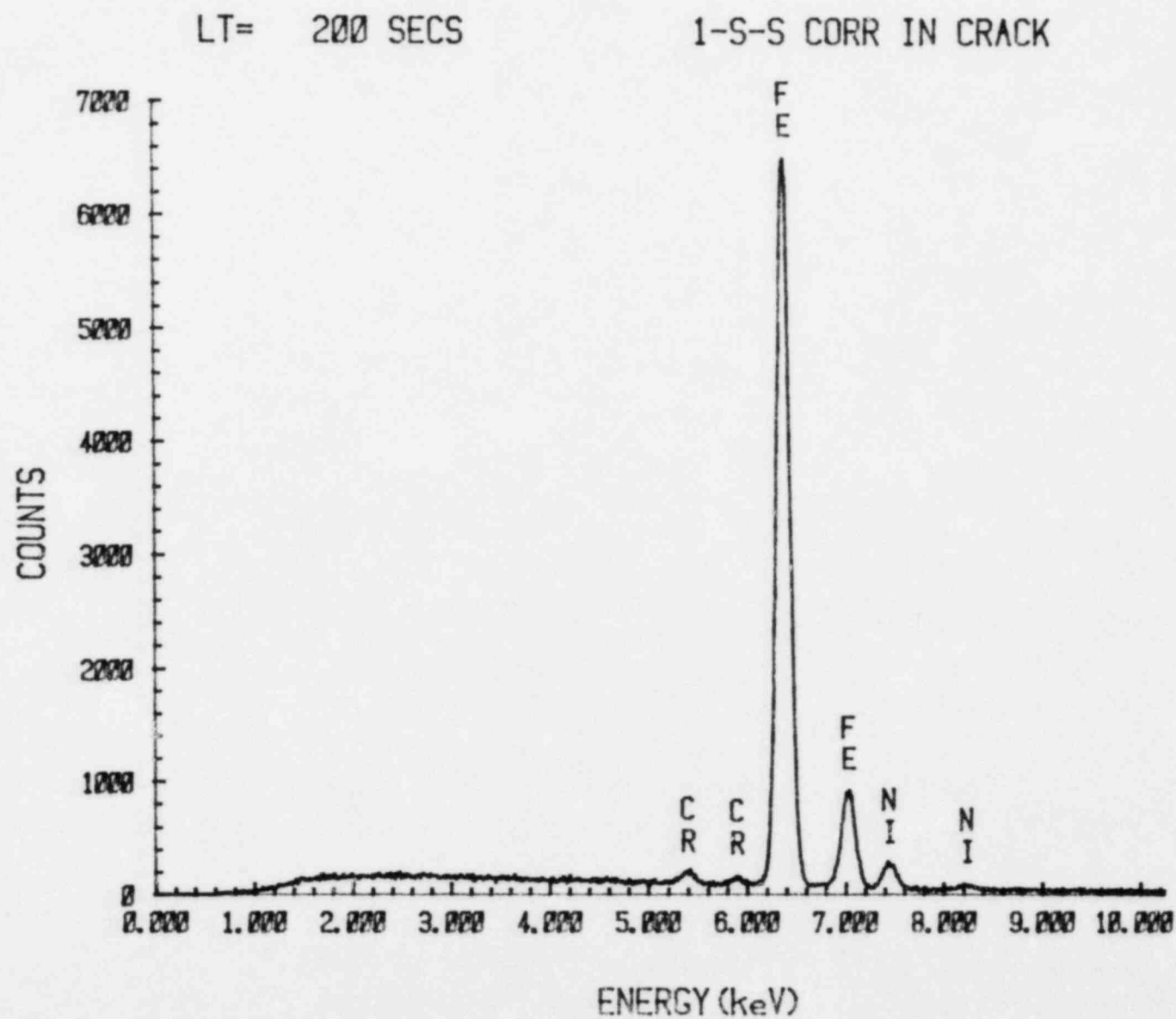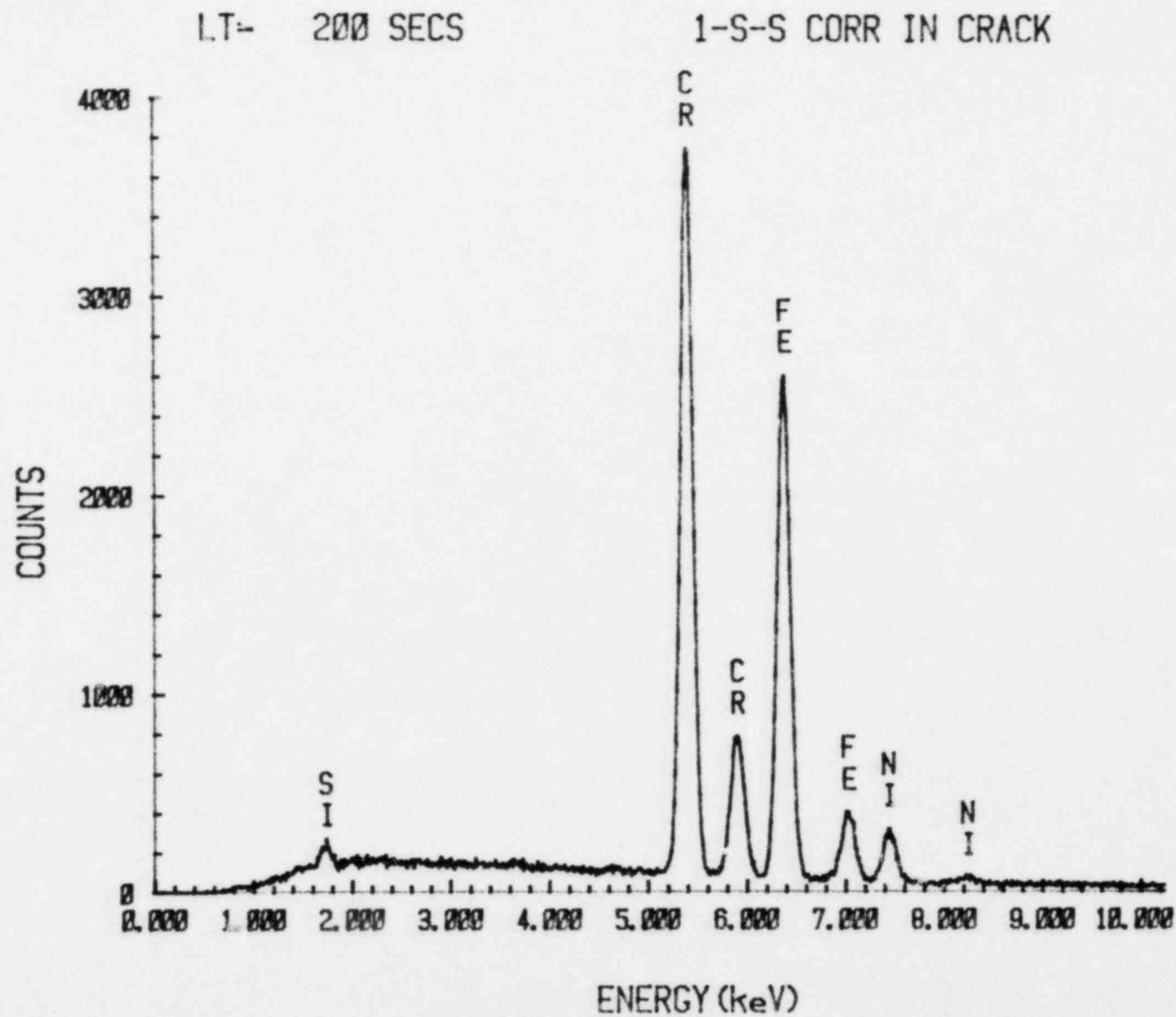
FIGURE 17. ENERGY-DISPERSIVE X-RAY SPECTRUM OBTAINED FROM AN ANALYSIS OF CORROSION PRODUCTS IN A BRANCH CRACK (AREA 6 IN TABLE 4)

chromium; the low chromium concentrations were similar to that found in the corrosion products in the main crack near the inside surface (Area 4 in Table 4).

A summary of the results presented in Table 4 indicates the following:

- The relative concentrations of nickel among the various corrosion products that were analyzed were on the order of 50 to 60 percent of the relative concentrations of nickel in the pipe or in the weld metal.
- The relative concentration of chromium in the corrosion products found along the principal IGSCC was significantly lower and the relative concentration of iron was significantly higher than those respective relative concentrations found in the pipe and in the weld metal.
- The relative concentrations of chromium and iron varied among the corrosion products in different branch cracks.
- The relative concentrations of iron, chromium, and nickel in the corrosion products in the surface flaw appeared to be similar to the concentrations of those elements in the corrosion products in branch cracks.
- The analyses of the pipe and the weld metal were similar, and they were nominally the same as the emission-spectrographic analyses obtained for those materials.

Corrosion Products in Flaw No. 2

The results of the EDAX electron-microprobe analyses of corrosion products observed within Flaw No. 2 are presented in Table 5. Those results were obtained from Specimen 2-N-N and Specimen 2-R-R of Flaw No. 2 (Specimen 2-N-N and Specimen 2-R-R of Flaw No. 2 are shown in Figures 9 and 10, respectively.)

Area 1 in Table 5 was located in the vicinity of the midlength of Flaw No. 2 with reference to Figure 9. The EDAX analysis of Area 1 was

TABLE 5. RESULTS OF SEMIQUANTITATIVE[a] ELECTRON-MICROPROBE
ANALYSES OF CORROSION PRODUCTS BY ENERGY-DISPERSIVE-
X-RAY ANALYTICAL TECHNIQUES IN SPECIMENS 2-N-N AND
2-R-R OF FLAW NO. 2

Area Analyzed	Relative Concentration of the Elements Detected[b], percent						
	Fe	Cr	Ni	Si	Al	Ti	S
Specimen 2-N-N (Figure 9)							
1 Midlength of the flaw (see Figure 19a)	67.1	19.6	8.5	0.8	2.5	0.7	0.8
2 Large particle in the center of Figure 19a	23.0	56.1	ND[c]	ND	15.8	5.2	ND
3 Another area near Area 1	68.4	5.8	18.8	0.6	0.6	ND	5.8
4 Tip of the flaw	72.1	14.7	10.5	1.8	0.6	ND	0.2
Specimen 2-R-R (Figure 10)							
5 Midlength of the flaw	66.4	21.6	9.2	1.0	1.8	ND	ND
6 Tip of the flaw	44.1	48.3	6.0	1.1	ND	ND	0.5

(a) The semiquantitative analysis is a standardless quantitative analysis of the X-ray-energy-spectra data that includes a full ZAF (atomic number, absorption, and fluorescence factors) matrix-correction calculation. The relative concentrations of the elements detected are normalized to obtain a sum of 1.0 (100 percent).

(b) Elements lighter than Atomic Number 11 (sodium) are not detected, so oxygen could not be determined.

(c) ND = not detected.

obtained by an area scan at a magnification of 2000X. The X-ray-energy
spectrum for Area 1 is presented in Figure 18; Area 1 is revealed in Figure
19a. Area 2 in Table 5 was a spot analysis of the large particle within
Area 1 that is visible in the center of Figure 19a. Nickel, silicon, and
sulfur were not detected in the large particle, whereas those elements, in
addition to iron, chromium, aluminum, and titanium, were detected within
Area 1 (Figure 19a) that included the particle. X-ray-distribution maps
of the elements detected in Area 1, except silicon, are presented in
Figures 19b through 19g. Figures 19f and 19g show, respectively, that the
nickel and sulfur were concentrated in a small particle, apparently nickel
sulfide, adjacent to the large particle.

The results presented in Table 5 seem to indicate that the compo-
sition of the corrosion products in Flaw No. 2 varies extensively from one
area to another. The elements usually detected in the different areas were
iron, chromium, nickel, aluminum, and silicon. Less frequently detected
elements were titanium and sulfur.

Corrosion Products in Flaw No. 5

The results of the EDAX electron-microprobe analyses of corrosion
products observed within Flaw No. 5 are presented in Table 6. Those results
were obtained from Specimen 5-U-U (Figure 11) of Flaw No. 5.

The principal elements detected in the corrosion products in
Flaw No. 5 were the same as those elements detected in the corrosion pro-
ducts in Flaw No. 1 and Flaw No. 2. As with those other flaws, variations
in the compositions of the corrosion products were evident among different
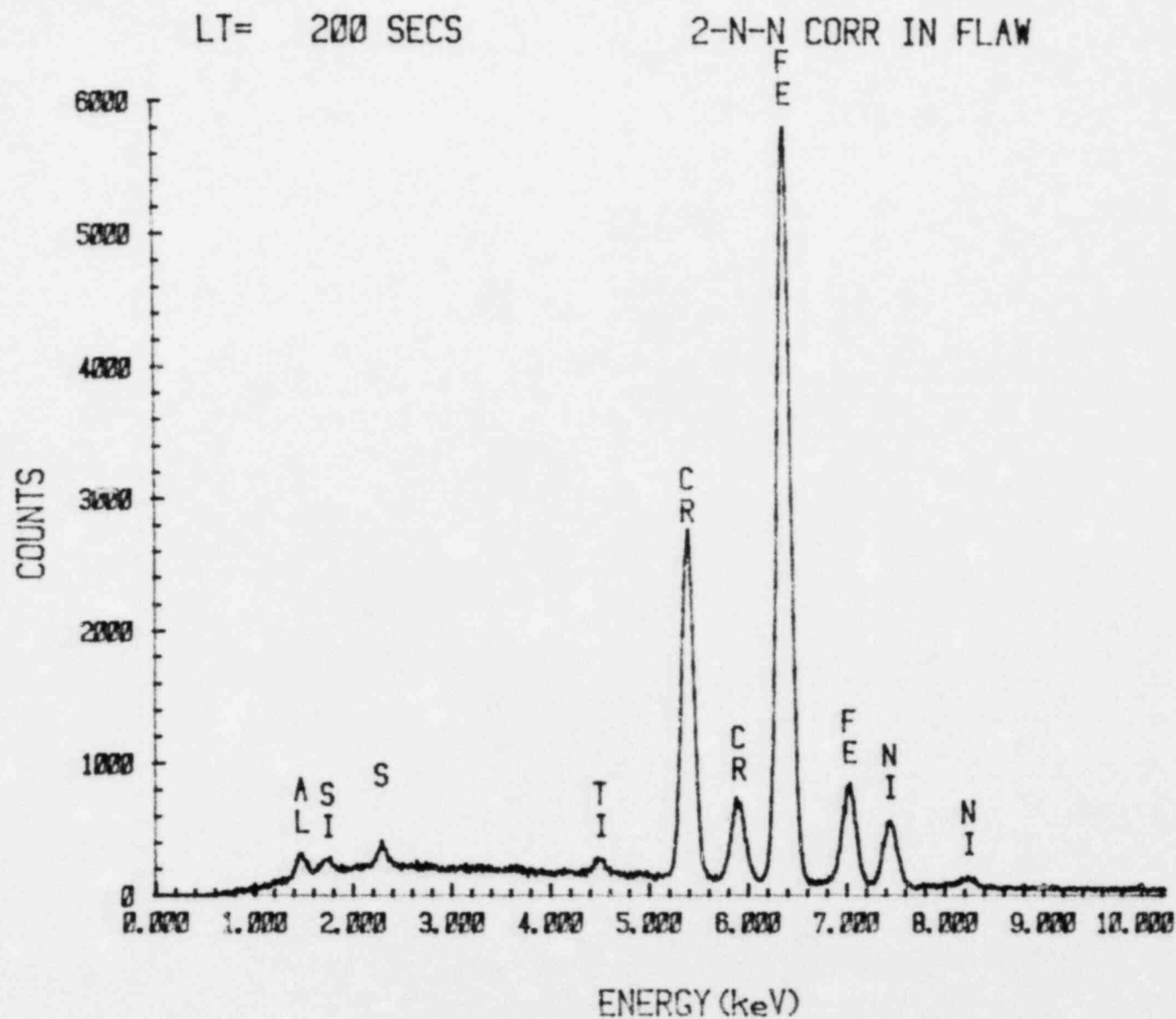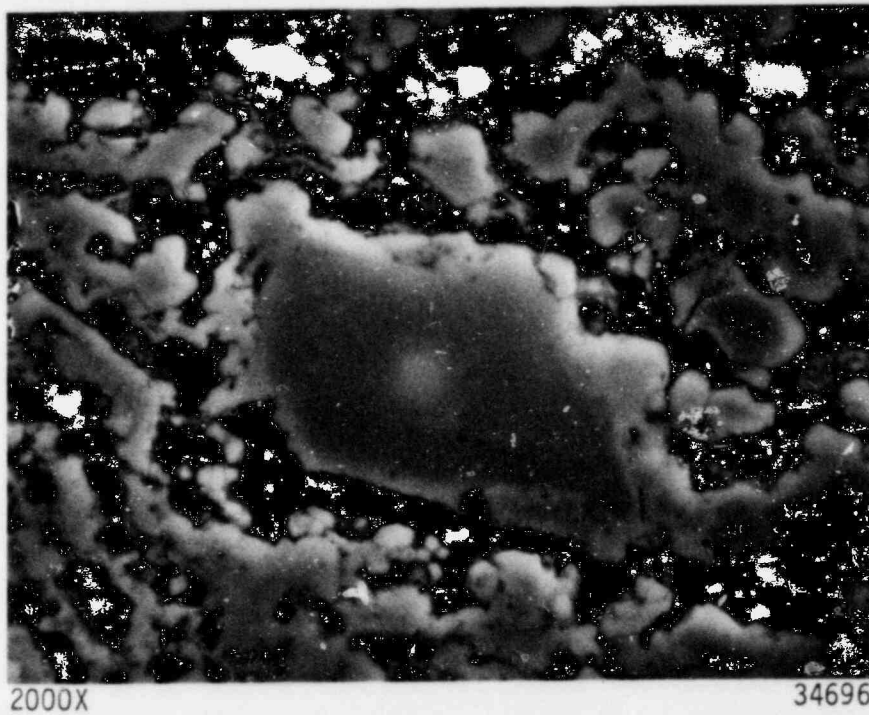areas that were analyzed.

FIGURE 18. ENERGY-DISPERSIVE X-RAY SPECTRUM OBTAINED FROM AN AREA SCAN OF CORROSION PRODUCTS IN FLAW NO. 2, SPECIMEN 2-N-N (AREA 1 IN TABLE 5)

2000X   34696

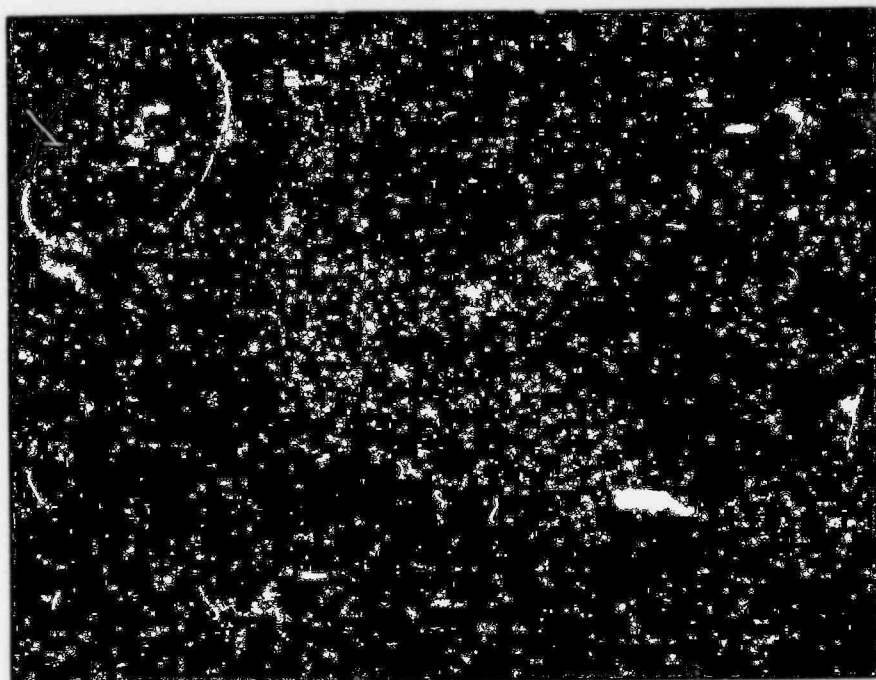a. Area 1 Reported in Table 5 (SEM Micrograph)

2000X   34699

b. X-ray-Distribution Map for Chromium in
   (a) Above

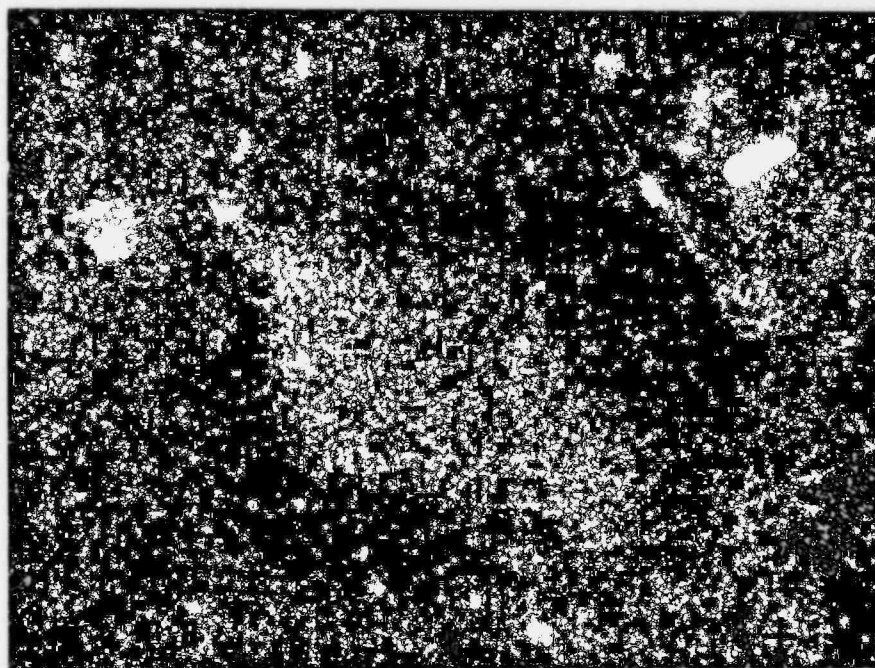FIGURE 19.   CORROSION PRODUCTS IN FLAW NO. 2 THAT WERE
             SUBJECTED TO ELECTRON-MICROPROBE ANALYSES

2000X   34700

c. X-ray-Distribution Map for Aluminum in (a) Above

2000X   34698

d. X-ray-Distribution Map for Titanium in (a) Above
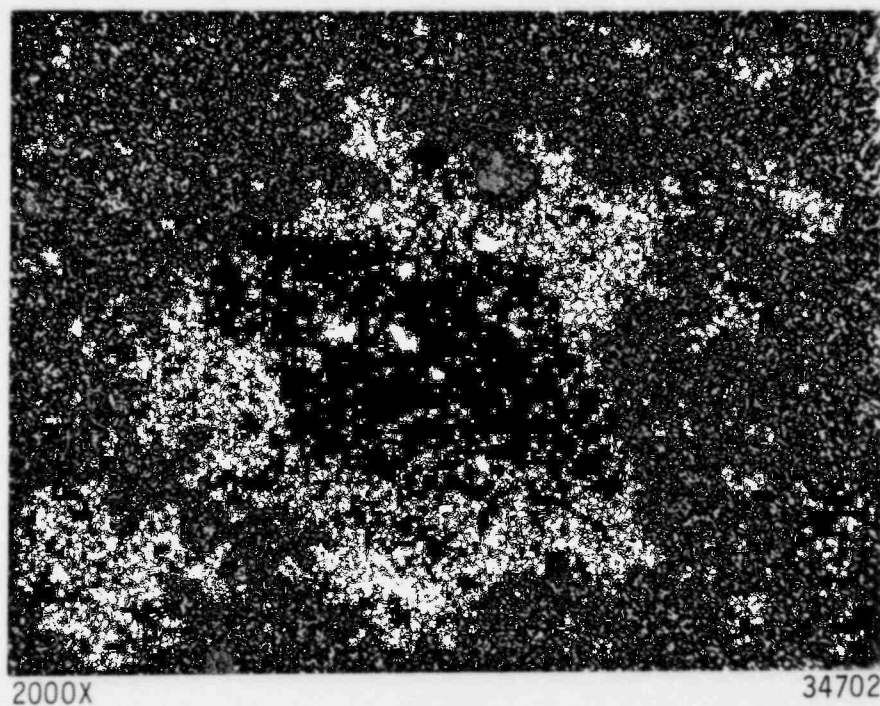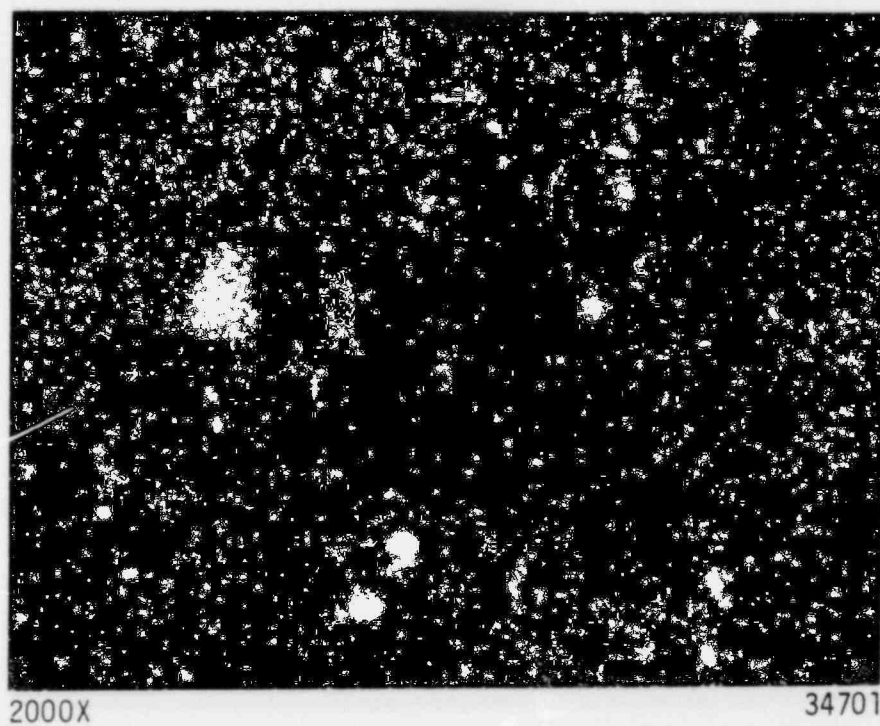
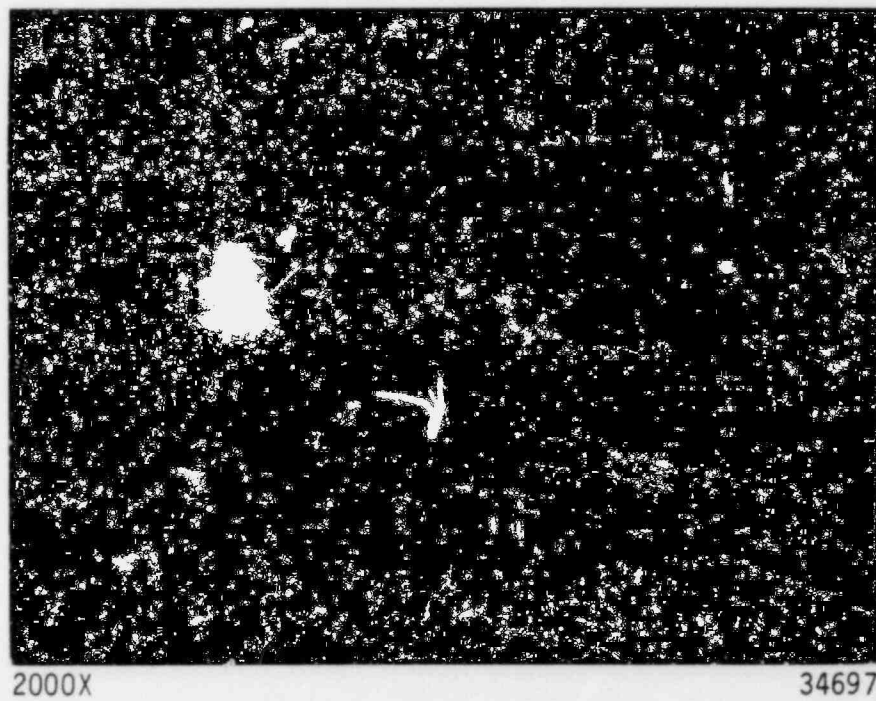FIGURE 19. (Continued)

2000X   34702

e.   X-ray-Distribution Map for Iron in (a) Above

2000X   34701

f.   X-ray-Distribution Map for Nickel in (a) Above

FIGURE 19.   (Continued)

2000X   34697

g. X-ray-Distribution Map for Sulfur in (a) Above

FIGURE 19. (Continued)

TABLE 6. RESULTS OF SEMIQUANTITATIVE[a] ELECTRON-MICROPROBE ANALYSES OF CORROSION PRODUCTS BY ENERGY-DISPERSIVE X-RAY ANALYTICAL TECHNIQUES IN SPECIMEN 5-U-U OF FLAW NO. 5

| Area Analyzed | Relative Concentration of the Elements Detected[b], percent | | | | | |
	Fe	Cr	Ni	Si	Al	S
1 Midlength of the flaw (see Figure 11)	86.9	2.3	9.1	1.5	ND[c]	0.3
2 Tip of the flaw	92.1	2.7	3.6	1.1	0.3	0.2

(a) The semiquantitative analysis is a standardless quantitative analysis of the X-ray-energy-spectra data that includes a full ZAF (atomic number, absorption, and fluorescence factors) matrix-correction calculation. The relative concentrations of the elements detected are normalized to obtain a sum of 1.0 (100 percent).

(b) Elements lighter than Atomic Number 11 (sodium) are not detected, so oxygen could not be determined.

(c) ND = not detected.

Electrochemical-Polarization-Reactivation (EPR) Tests

The EPR test* was developed by General Electric Company as a means to reveal the susceptibility of austenitic stainless steel piping to inter-granular stress-corrosion cracking (IGSCC) in nuclear applications. The need for such a test arose from major problems in the past in the nuclear power industry with IGSCC in the weld-heat-affected zones of Type 304 stainless steel primary-coolant piping. The corrodent has been high-purity water that contained less than 9 ppm oxygen and less than C.3 ppm chloride.

---

* Clarke, W. L., et al, "Detection of Sensitization in Stainless Steel Using Electrochemical Techniques", Paper 180, in Corrosion '77, National Association of Corrosion Engineers, Houston, Texas (1977).

Cihal, V., "A Potentiokinetic Reactivation Method for Predicting the I.G.C. and I.G.S.C.C. Sensitivity of Stainless Steels and Alloys". Corrosion Science, 20, 737 (1980).

In the EPR test, a stainless steel specimen, in a strong acid
electrolyte, is cathodically cleaned and then held at an anodic potential
to passivate the surface. The potential is then shifted in the cathodic
direction through the corrosive range to test the passivating film produced
previously. The resulting corrosion current during this shift (electro-
chemical reverse scan) is indicative of the degree of protection provided
by the prior passivation treatment. A protective film will yield only a
very small corrosion current, whereas a poorly protective film, such as
the film over the chromium-depleted region adjacent to grain-boundary
chromium carbides in a sensitized stainless steel, will yield a large cor-
rosion current in the reverse scan. The ratio of the maximum corrosion
current during the cathodic scan to the maximum corrosion current during
the original anodic scan (EPR ratio) is used as a measure of the degree of
sensitization. Limited experience has indicated that austenitic stainless
steels having corrosion-current ratios of less than 0.04 in the EPR test
are not sensitized and are not susceptible to intergranular cracking. More-
over, past experience with cast AISI 316 stainless steel indicated that
material with an EPR ratio of approximately 0.01 was not susceptible to
IGSCC, whereas material with EPR ratios that exceeded about 0.08 were sus-
ceptible. At the present time, a definite threshold value of the EPR ratio
for the occurrence of IGSCC cannot be defined and probably varies with
material.

The EPR tests were conducted during this investigation as a means
of evaluating the degree of sensitization in the weld heat-affected zone and
at the inside and outside surfaces of the subject pipe away from weld-heat
effects. The initial EPR tests were made using an electrolyte that consisted
of 2M H_2SO_4 and 0.1M KCL. Those tests showed no evidence of sensitization
in either the weld-heat-affected-zone sample, EPR-2 in Figure 1, or the
pipe samples, EPR-1 1D and EPR-1 OD, remote from the welded region. A
review of the literature indicated that the electrolyte was probably too
weak. The EPR tests were repeated, therefore, in an electrolyte that con-
sisted of 2M H_2SO_4 and 0.5M KCl.

The results of the tests performed in the stronger solution are
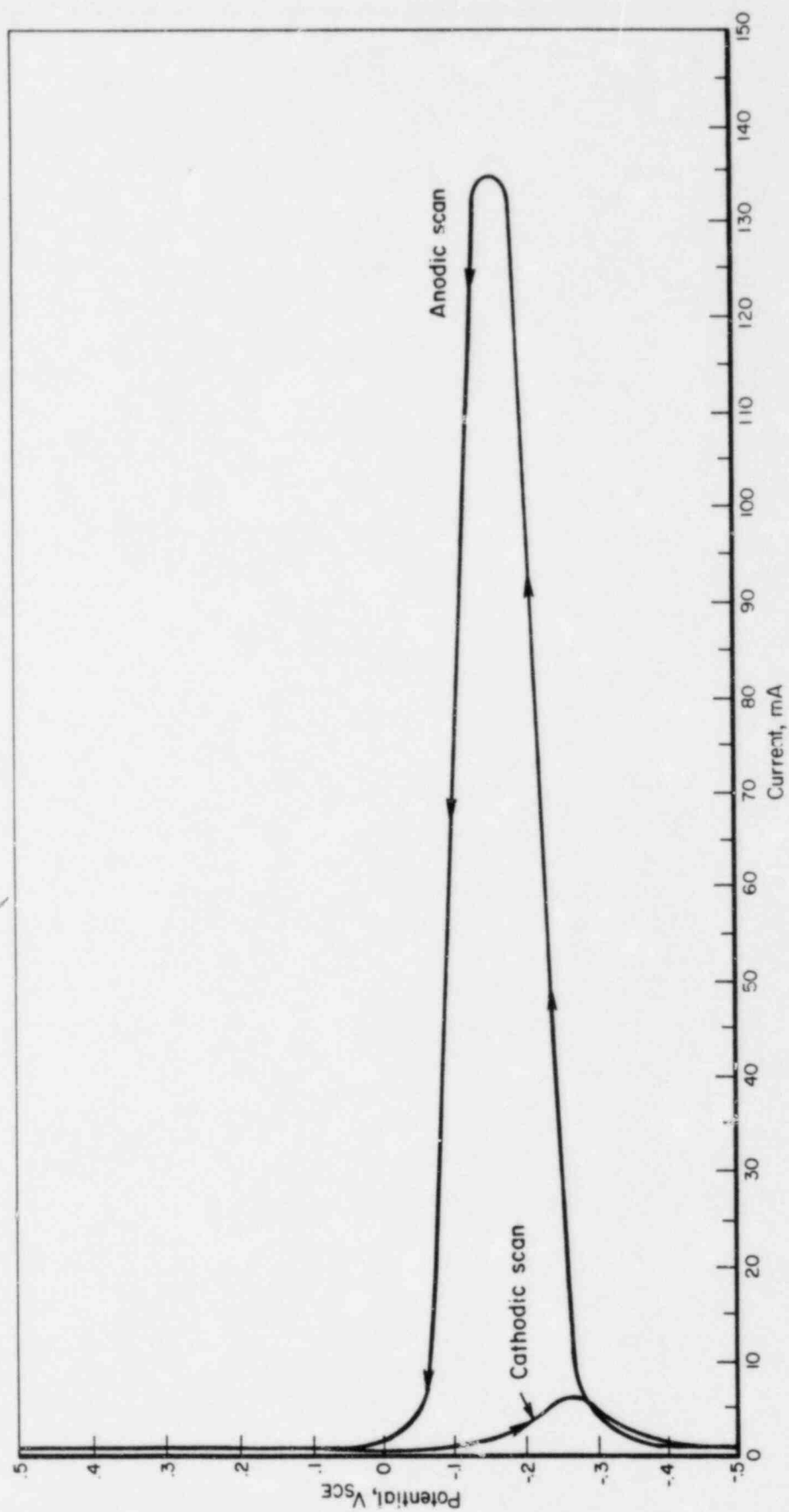revealed in Figures 20 and 21 by a plot of current, mA, versus saturated

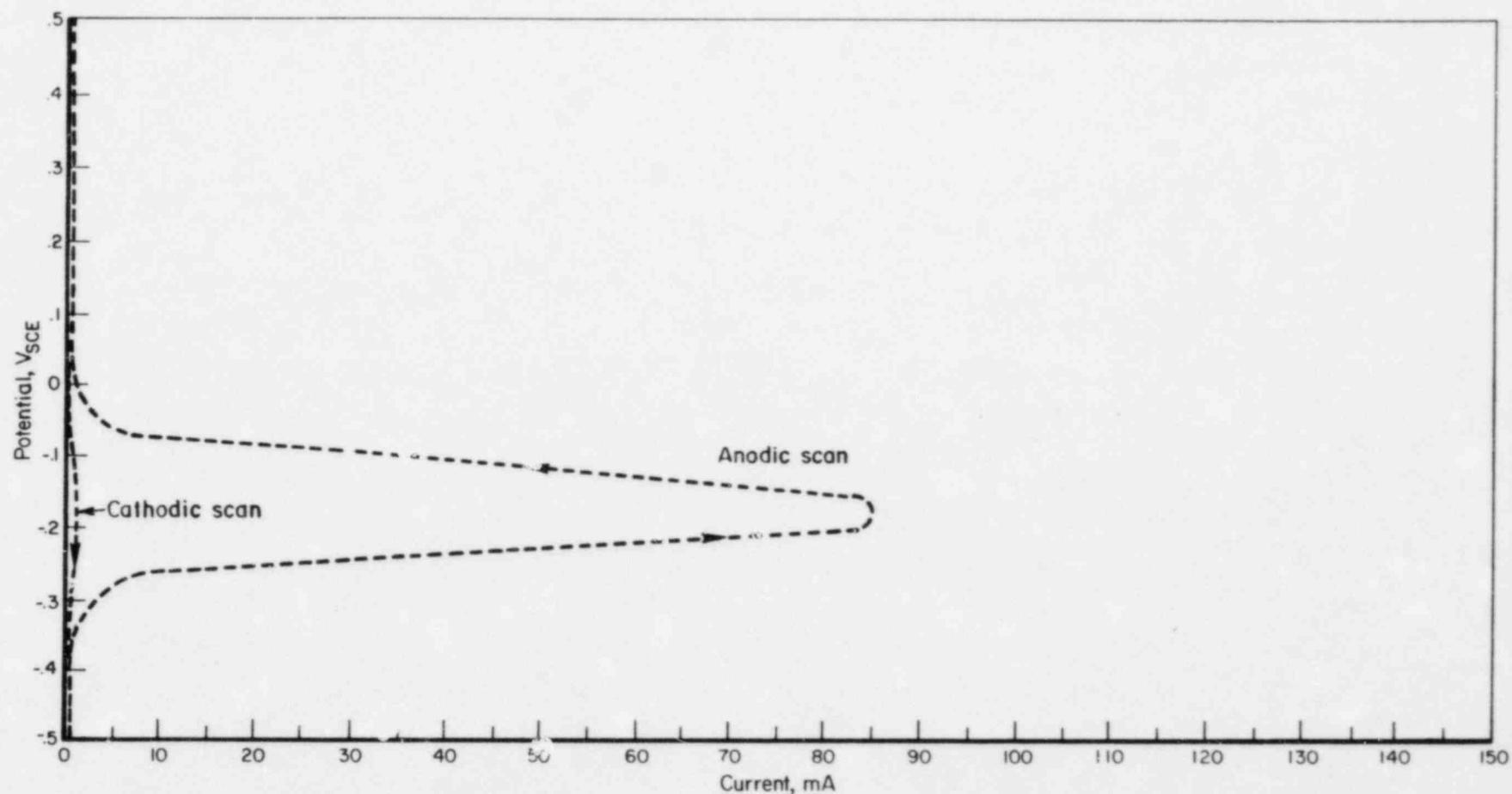FIGURE 20. EPR CURVES FOR SAMPLE EPR-2 FROM THE WELD HEAT-AFFECTED ZONE

FIGURE 21. EPR CURVES FOR SAMPLES EPR-1 ID AND EPR-1 OD, AISI 304 STAINLESS STEEL PIPE REMOTE FROM THE REGION OF THE WELD

The same curve was obtained for both samples.

calomel electrode potential, V_{SCE}. For the weld heat-affected zone, the ratio of the maximum corrosion current during the cathodic scan to the maximum corrosion current during the original anodic scan was calculated to be 0.048 (Figure 20); the EPR ratio for the pipe samples remote from the welded region was calculated to be 0.009 (Figure 21). Thus, the weld heat-affected zone adjacent to the weld was more susceptible to IGSCC than was the stainless steel pipe. The higher susceptibility to IGSCC of the heat-affected zone apparently was a result of the sensitized condition of that zone.

DISCUSSION

The investigation of surface flaws revealed evidence similar to that reported in the earlier metallographic examinations, namely, evidence that the surface flaws were introduced during the production of the seamless pipe. The evidence indicated further that the fabrication-induced flaws were similar to laps or seams. Such flaws probably originated during the piercing operation.

IGSCC's were found to be associated with flaws that were located in the region of the girth-weld heat-affected zone; IGSCC's were not observed at flaws located outside the heat-affected zone. Metallographic examination revealed that the weld heat-affected zone had been sensitized. Based on the results of the EPR tests, the presence of IGSCC's in the weld heat-affected zone is not unexpected. The sensitized condition of the weld heat-affected zone apparently caused the zone to possess a degree of susceptibility to IGSCC, as was indicated by the EPR-test results; in the parent metal outside the heat-affected zone, no degree of susceptibility of the pipe to IGSCC was indicated. However, evidence of IGSCC was not observed in regions of the heat-affected zone where surface flaws were absent. Thus the presence of a surface flaw in the region of the heat-affected zone was apparently a major factor that contributed to the initiation of IGSCC. The contribution of the surface flaw to the onset of IGSCC was most likely in the manner of a stress raiser.

The profiles of the IGSCC's indicated that the major portions of the IGSCC surfaces were within the sensitized region underneath the surface flaws. The extremities of the cracks extended short distances beyond the ends of the flaws that were observed on the inside surface of the pipe. The depth of one crack below the inside pipe surface extended nearly through the thickness of the pipe wall and the other crack apparently penetrated the wall. For the most part, the propagation of the cracks appeared to be arrested in the through-wall direction by the broad, final passes of weld metal on the outside pipe surface and, in the pipe-axis direction, by the welded zone through the pipe wall at one end of the crack, and by the non-sensitized parent metal at the other end of the crack.

The electron-microprobe analyses of corrosion products in the surface flaws and in the IGSCC's did not identify the presence of a specific corrodent. Most likely the corrodent was the water in the core-spray system that contained low concentrations of oxygen and perhaps chloride that could not be detected by energy-dispersive X-ray analysis.

CONCLUSIONS

The results of the investigation led to the following conclusions:

- Linear indications on the inside pipe surface were fabrication-induced surface flaws.
- IGSCC was associated only with surface flaws that were located in the region of a sensitized weld heat-affected zone.
- Surface flaws acting as stress raisers were a major factor that led to the initiation of IGSCC.
- In the weld heat-affected zone, the IGSCC's extended through most of the pipe wall.
- Propagation of IGSCC was apparently arrested by weld metal and nonsensitized parent metal that surrounded the weld heat-affected zone.
- In the absence of the fabrication-induced surface flaws, IGSCC may not have occurred in the weld heat-affected zone.